9

ENSO Modeling: History, Progress, and Challenges

Eric Guilyardi[1], Antonietta Capotondi[2], Matthieu Lengaigne[3], Sulian Thual[4], and Andrew T. Wittenberg[5]

ABSTRACT

Climate models are essential tools for understanding ENSO mechanisms and exploring the future, either via seasonal-to-decadal forecasting or climate projections. Because so few events are well observed, models are also needed to help reconstruct past variability, explore ENSO diversity, and understand the roles of the background mean state and external forcings in mediating ENSO behavior. In this chapter we review the history of ENSO modeling, showing the gradual improvement of models since the pioneering studies of the 1980s and 1990s and describing the existing hierarchy of model complexity. The rest of the chapter is devoted to coupled general circulation models (GCMs) and how these models perform, related model development and improvements, associated systematic biases and the strategies developed to address them, and methods of model evaluation in a multimodel context with reference to observations. We also review how successive generations of multimodel intercomparisons help bridge the gap between our theoretical understanding of ENSO and the representation of ENSO in coupled GCMs. Much of the improved understanding of ENSO in recent decades, addressed in other chapters of this monograph, was obtained from simulation strategies in which part of the coupled ocean-atmosphere system was either simplified or omitted, such as atmosphere-only, ocean-only, partially coupled, or nudged simulations. We here review these strategies and the associated best practices, including their advantages and limitations. The ability of coupled GCMs to simulate ENSO continues to improve, offering exciting opportunities for research, forecasting, understanding past variations, and projecting the future behavior of ENSO and its global impacts. We list the challenges the community is facing, as well as opportunities for further improving ENSO simulations.

9.1. HISTORY OF ENSO SIMULATION IN COMPLEX MODELS

From their initial development at the end of the 1960s, early coupled general circulation models (GCMs) remained relatively crude up to the 1990s, with coarse resolution, limited physical parameterizations, and strongly biased air-sea surface fluxes. Model drift from the observed mean state was often substantial, and their use for investigating climate variability such as ENSO was very limited. The Tropical Ocean–Global Atmosphere (TOGA) program was a milestone that allowed substantial progress in ENSO understanding and modeling, in particular via improved parameterizations; see also chapter 1. This program led to the first comprehensive review of ENSO in a special edition of *Journal of Geophysical Research: Oceans* (https://agupubs.onlinelibrary.wiley.com/doi/toc/10.1002/(ISSN)2169-9291.TOGA1 and Delecluse et al., 1998). Within a few years, improved model resolution and physics led to the natural occurrence of ENSO in coupled GCMs.

[1] *LOCEAN-IPSL, CNRS/Sorbonne University/IRD/MNHN, Paris, France; and NCAS-Climate, University of Reading, Reading, UK*

[2] *University of Colorado, CIRES, Boulder, CO, USA; and NOAA Physical Sciences Laboratory, Boulder, CO, USA*

[3] *LOCEAN-IPSL, Sorbonne Universités/UPMC-CNRS-IRD-MNHN, Paris, France; and MARBEC, University of Montpellier, CNRS, IFREMER, IRD, Sète, France*

[4] *Institute of Atmospheric Sciences/Department of Atmospheric and Oceanic Sciences, Fudan University, Shanghai, China*

[5] *NOAA Geophysical Fluid Dynamics Laboratory, Princeton, NJ, USA*

El Niño Southern Oscillation in a Changing Climate, Geophysical Monograph 253, First Edition.
Edited by Michael J. McPhaden, Agus Santoso, and Wenju Cai.

Studies of coupled models began to reveal biases that had been concealed in the ocean-only or atmosphere-only simulations used up to then. A community of scientists, working at the interface between the ocean and the atmosphere, steadily grew and now forms the core of ENSO expertise in the tropics.

A series of coupled model intercomparison projects (CMIPs) have shown steady progress in simulating ENSO and related global variability using state-of-the-art coupled GCMs (AchutaRao & Sperber, 2006; van Oldenborgh et al., 2005; Guilyardi 2006; Capotondi et al., 2006; Wittenberg et al., 2006; Bellenger et al., 2014; C. Chen et al., 2017). Improvements in model formulation and resolution have led to better representation of many key features of ENSO; see 4th and 5th assessment reports of the Intergovernmental Panel on Climate Change (IPCC AR4 and AR5) and the *Special Report on the Ocean and Cryosphere in a Changing Climate*. In contrast to the 1990s, progress in the past two decades has been gradual. A number of studies nevertheless have pointed to key factors essential to a realistic simulation of ENSO in a coupled GCM, in particular, properly representing deep convection and clouds in the atmospheric component (which depends to a large extent on the atmospheric horizontal grid resolution), and properly representing equatorial wave dynamics, upwelling, and vertical mixing in the oceanic component (a strong function of oceanic grid resolution, especially in the meridional and vertical directions near the equator). The CMIP5 models showed progress relative to their CMIP3 counterparts, as all CMIP5 models displayed some kind of ENSO-like behavior. However, the best CMIP5 models were only marginally better than the best CMIP3 models. CMIP5 also included models with increased nonlinear behavior, stemming mostly from better-resolved atmospheric processes, such as convective thresholds or the ability to simulate intraseasonal variability like the Madden-Julian Oscillation (MJO) and westerly wind bursts (WWBs, also known as westerly wind events or WWEs). Yet as detailed in section 9.4, systematic errors still persist, decades after their first identification.

In the early 2000s, once models were able to simulate ENSO properties (e.g. amplitude and frequency) closer to observed, model evaluation began to include process-based metrics to ensure that the right properties were simulated for the right reasons and not via error compensation (Guilyardi et al., 2004, Kim & Jin, 2011). Besides providing invaluable feedbacks to model developers, multimodel intercomparisons continue to help bridge the gap between theoretical understanding of El Niño and its representation in coupled GCMs (CGCMs) (Fedorov et al., 2003; Held 2005; Kim & Jin, 2011). Hence, thanks to this improved theoretical understanding of ENSO, more mature diagnostic tools are now available to help unravel the underlying ENSO mechanisms. ENSO model evaluation has grown into a very active area of research, and exciting steps lie ahead.

9.2. BENEFITS OF A HIERARCHY OF MODELS

A hierarchy of models of increasing complexity has made it possible to simulate, experiment with, and understand the dynamics of ENSO. This hierarchy includes (i) simple oscillators, which describe the cyclic nature and essential parameters of the phenomenon; (ii) intermediate models, which describe the fluid dynamics and thermodynamics of the equatorial ocean and atmosphere with some simplifications; and (iii) GCMs, which describe global climate with as much resolution and comprehensiveness as possible on the world's most powerful supercomputers. Each type of model serves different goals and has its own advantages and requirements. The simplest models can capture novel theoretical concepts, highlight specific mechanisms, are valuable teaching tools, and have served as sources of insight into ENSO sensitivities and sources of predictability. The simple models are easily understood, tractable, and versatile, at the cost of being mostly qualitative, limited in focus, and sometimes difficult to relate directly to observations. In contrast, general circulation models are much more detailed as they attempt to account for the full complexity of the climate system; however, due to their complexity, such models are expensive to maintain and improve and more difficult to diagnose and understand.

There are also important advantages in working simultaneously with models of different levels of complexity. Simple models can often be used to interpret GCMs and understand their biases via process-based metrics (e.g. An & Jin, 2004; Jin et al., 2006; Brown et al., 2011; K.-Y. Choi et al., 2013, 2015; Graham et al., 2015; Vijayeta & Dommenget, 2018). For example, the Bjerknes stability index, a process-based metric derived from the recharge oscillator paradigm, has allowed the identification of errors in the GCMs (Kim & Jin, 2011), with some caveats (Graham et al., 2014). Conversely, the full characterization of ENSO's behavior gained from GCMs can inform the development of simpler conceptual models. For instance, many studies adopt a hybrid approach where GCM outputs infer the parameters or characteristics of a simpler model that is then analyzed more extensively due to its lower computational cost. Finally, the above hierarchy is flexible to some extent, because models sometimes couple components of vastly different complexity (e.g. an ocean GCM to a statistical atmosphere, etc.). Comprehensive coupled GCMs have been described in many places (Flato et al., 2013; Guilyardi et al., 2009), so we focus in this section on the simpler range of the model hierarchy.

9.2.1. Harmonic Oscillator Models

The simplest ENSO models are harmonic oscillators constructed from ordinary differential equations that capture the oscillatory nature of ENSO with periods of 2 to 7 years. Several harmonic oscillator models have been proposed. They all share a similar mathematical form but differ greatly in the variables and processes described, as well as in the approximations made to represent the oceanic and atmospheric dynamics (e.g. Picaut et al., 1997; Clarke et al., 2007). One example is the recharge/discharge oscillator model (Jin, 1997), which in its simplest form (Burgers et al., 2005) is expressed as

$$\begin{aligned} \frac{dT}{dt} &= aT + b\,H \\ \frac{dH}{dt} &= c\,H + dT, \end{aligned} \tag{9.1}$$

where T is a spatial average of sea surface temperature anomalies (SSTAs), H is a spatial average of thermocline depth anomalies, and a, b, c, d are fixed parameters. Another example is the delayed oscillator (Suarez & Schopf, 1988; Battisti & Hirst, 1989), which reads in its simplest form

$$\frac{dT}{dt} = f\,T - g\,T\left(t-\tau\right), \tag{9.2}$$

where τ is a fixed delay and f, g are fixed parameters (see chapter 6 for further details).

These models typically include a fast positive feedback that results in the growth of El Niño SSTAs, as well as a delayed negative feedback responsible for reversing the phase of the oscillation. While the positive feedback in most models is a representation of the Bjerknes feedback, the nature of the negative feedback may vary from model to model. For instance, the delayed oscillator above emphasizes the delayed propagation and reflection of oceanic equatorial waves, while the recharge/discharge model emphasizes the meridional transport of equatorial heat content. While all of those processes seem to be at work in the real world, none of them is sufficient to provide a complete picture of ENSO mechanisms (Wang & Picaut, 2004). Furthermore, many of these conceptual models have struggled to capture the full behavior of ENSO seen in observations or coupled GCMs (Graham et al., 2014, 2015).

Despite those drawbacks, harmonic oscillators have proven to be an invaluable testbed for theoretical concepts of more advanced features of ENSO dynamics. In fact, basic modifications of the equations above produce more realistic ENSO evolution. For example, the addition of fundamental nonlinearities mimics the observed bursting nature of ENSO, its asymmetry between El Niño and La Niña, and distinct strong and moderate regimes of evolution (e.g. Timmerman & Jin, 2003; Guckenheimer et al., 2017; Takahashi et al., 2018). Similar features may also be obtained through the addition of stochastic noise, which parameterizes fast atmospheric wind bursts and their dependence on sea surface temperatures (SSTs; Jin et al., 2007; Levine & Jin, 2010, Bianucci et al., 2018). Other modifications lead to seasonal synchronization of ENSO (e.g. Stein et al., 2014). Although these descriptions remain limited in scope, they provide intuitive illustrations of fundamental aspects of ENSO, involving its causes, evolution, and predictability. They also depict to a reasonable extent the dynamical regimes found in more complex models, thanks to the inherent low-order nature of ENSO (Karamperidou et al., 2014).

9.2.2. Linear Inverse Modeling

Besides simple models developed to represent key dynamical ENSO feedbacks, there are "empirical dynamical" models that estimate the model operators directly from the data. Linear inverse models (LIMs) have been extensively used to understand and predict ENSO (Penland & Sardeshmukh, 1995). In the LIM framework, the tropical Pacific is described in terms of an anomaly state vector $\boldsymbol{x}$, which is constructed from anomalies of the key system variables. The evolution of $\boldsymbol{x}$ is then modeled in terms of linear, damped, stochastically perturbed dynamics (Penland & Sardeshmukh, 1995; Newman et al., 2011) of the form

$$d\boldsymbol{x} = L\,\boldsymbol{x}\,dt + \boldsymbol{S}\mathbf{r}\sqrt{dt}, \tag{9.3}$$

where the linear operator $\boldsymbol{L}$ encapsulates the predictable dynamics of the system, the matrix $\boldsymbol{S}$ represents spatially coherent stochastic forcing patterns, and $\mathbf{r}$ is a vector of random numbers drawn from a normal distribution with zero mean and unit standard deviation. The operators $\boldsymbol{L}$ and $\boldsymbol{S}$ can be estimated directly from the covariance matrices of $\boldsymbol{x}$.

The leading eigenvectors of the $\boldsymbol{L}$ operator, known as empirical normal modes, are nonorthogonal and damped, with some of them having an oscillatory component. Thus, ENSO can be effectively described as a damped oscillatory phenomenon, governed by (predominantly) linear dynamics, and energized by atmospheric stochastic forcing. This is a very different paradigm than those proposed in many seminal ENSO studies (Philander et al., 1984; Zebiak & Cane, 1987; Schopf & Suarez, 1988, 1990; Neelin & Jin, 1993, among others), which viewed ENSO growth as the result of a dynamical instability (involving unstable mode(s) and no need for stochastic forcing). In addition, if ENSO can be described by a subset of the empirical normal modes which evolve over time, the implication is that ENSO cannot be merely identified

with its mature state but should be viewed, instead, as an evolving phenomenon that grows from some initial condition (the ENSO precursors) to a mature stage, followed by a decay phase. Apart from providing insights into the nature of ENSO, the empirical dynamical model (9.3) can be integrated in time for several millennia and provide very long synthetic time series of the key system variables. These time series encapsulate the statistics of the system and can be used to assess the statistical significance of observed (or modeled) ENSO changes (Capotondi & Sardeshmukh, 2017). To reduce the number of degrees of freedom, only a limited number of variables are usually included in the LIM state vector. Although the covariance matrices used to compute the dynamical operator $\boldsymbol{L}$ incorporate the dynamical feedbacks of the system, dynamical processes are not explicitly represented in the LIM approach, somewhat limiting the interpretability of the LIM results in terms of conventional diagnostic methods.

9.2.3. Models of Intermediate Complexity

Next in the hierarchy of ENSO models are Earth models of intermediate complexity (EMICs). EMICs use heavily parameterized processes to explicitly depict the spatial and temporal evolution of the climate system (Claussen et al., 2002), though with much less detail than full three-dimensional GCMs.

The ocean-atmosphere dynamics and SST thermodynamics in EMICs have substantial simplifications, though they retain the processes deemed essential for the ENSO (Zebiak & Cane, 1987; Battisti & Hirst, 1989). Typically, EMICs are two-dimensional (2D) models where the flow depends on longitude, latitude, and time while the vertical structure is fixed in the ocean and atmosphere. This 2D representation of the flow (two spatial dimensions in addition to time) has the advantage of being simpler to deal with than the usual 3D representation. EMICs are formulated as anomaly models, that is, they describe departures from prescribed basic state conditions (e.g. the annual mean and seasonal cycle). They commonly adopt the shallow water approximation for the ocean component, which assumes an active upper layer separated from the resting deep ocean by a well stratified thermocline (which is equivalent to retaining only the first vertical baroclinic mode). The atmosphere may also be described by shallow water dynamics for a single vertical layer, treated as a fast adjusting component compared to the ocean, and admitting steady state solutions (e.g. Gill, 1980). Heating from deep convection is parameterized according to empirical relationships (Kleeman, 1993), or the atmosphere can be entirely derived from statistical relationships between surface wind stress and the ocean state (Latif & Villwock, 1990; Barnett et al., 1993; Syu et al., 1995; Wittenberg, 2002; Vecchi et al., 2006). Finally, a thermodynamic budget for SST in the ocean mixed-layer is systematically included.

While EMICs usually consist of the above main ingredients (e.g., Zebiak & Cane, 1987; Neelin et al., 1998), their complexity ranges widely from simple models to GCMs. One of the simplest class of EMICs are zonal strip models, i.e. 1D models whose evolution depends only on longitude and time thanks to a meridional truncation, where the flow is either confined to an equatorial strip or Galerkin-projected on the first meridional parabolic cylinder functions (e.g., Jin & Neelin, 1993; An & Jin, 2001; Jin, 2001; Thual et al., 2016). These zonal strip models explicitly account for the propagation and reflection of equatorial ocean waves and therefore capture both the recharge/discharge and delayed oscillator mechanisms of ocean adjustment described by the harmonic oscillators in section 9.2.1. Of much higher complexity, closer to CGCMs, are hybrid coupled models. These typically consists of a simplified dynamical or statistical atmosphere coupled to an ocean GCM that includes important details of the 3D vertical structure, as well as small-scale and nonlinear processes (e.g., Neelin, 1990; Barnett et al., 1993; Syu et al., 1995; Wittenberg, 2002). Another (less common) type of hybrid coupled model instead couples a simplified ocean model to an atmospheric GCM (e.g., Kirtman & Zebiak, 1997; Yu et al., 2015). Some EMICs even include biogeochemical processes that can feed back on ENSO (e.g. Marzeion et al., 2005; R. Zhang et al., 2019).

EMICs have been very popular in the past, achieving for example the first successful forecast of the 1986/87 El Niño (Zebiak & Cane, 1987). Despite today's more widespread use of CGCMs, EMICs still remain widely used for targeted applications; this is mostly due to EMICs' considerably lower computational cost, and because EMICs facilitate understanding and control of the simulated ENSO processes. EMICs may be tools of choice, e.g., for sensitivity or large ensemble experiments, as well as for very long simulations where their design helps avoid the long-lasting problem of climate drifts found in most CGCMs. Following their extensive use in pioneering studies on ENSO predictability (e.g. Kleeman & Power, 1994; D. Chen et al., 1995) and seasonal prediction (Barnett et al., 1993; D. Chen et al., 2004; R.-H. Zhang et al., 2003), EMICs also remain routinely used for operational forecasts. Their skill in forecasting ENSO is overall similar to that of other models including GCMs, with the exception of a few advanced prediction systems (Barnston et al., 2012). Finally, EMICs have contributed to the understanding of ENSO dynamics, including, among others, the nature of ENSO's coupled instabilities (Jin & Neelin, 1993), the role of mixed-layer thermodynamical feedbacks (An & Jin, 2001), and ENSO interactions with the basic state (An & Wang, 2000; Fedorov & Philander,

2001; Wittenberg, 2002) or the seasonal cycle (Tziperman et al., 1994). Although most EMICs do not explicitly resolve fast and small-scale atmospheric variability such as wind bursts, some of them include ad-hoc representations or stochastic parameterizations that illuminate the impacts of atmospheric noise on ENSO characteristics, dynamics, and predictability (e.g. Moore & Kleeman 1999; Eisenman et al., 2005; Gebbie et al., 2007; Zavala-Garay et al., 2008; Thual et al., 2016).

9.3. USING MODELS FOR ENSO UNDERSTANDING

Climate models are therefore essential tools for understanding ENSO mechanisms and exploring the future, either via seasonal/decadal forecasting or climate projections (chapters 10 and 13). Because so few events are well observed, models also help to reconstruct past variability and explore the influence of external forcing (chapters 5, 11–13). Early on, the variety of ENSO behaviors exhibited by coupled models provided evidence that more than one mechanism was active in the generation and evolution of ENSO events (chapters 6 and 7). Much research has since been devoted to describing the mechanisms involved and, more recently, to understanding their relative balance, as well as the time variations of this balance. Models were also instrumental in showing that interannual variability is linked to the mean/decadal structure of the equatorial Pacific (chapter 8), and this opened up the exploration of the factors that affect the mean state, such as external forcing, vs. the impact of internal variability at multiple timescales (from intraseasonal to multidecadal).

Much of this new knowledge on ENSO was obtained from sensitivity simulations in which part of the coupled ocean-atmosphere system was either simplified or omitted, such as atmosphere-only GCM (AGCM), ocean-only GCM (OGCM), and partially coupled or nudged models. Coordinated sensitivity simulations (e.g. MIPs; Eyring et al., 2016, and https://explore.es-doc.org/) are now a common way to explore the robustness of the mechanisms found. Experience indeed shows that drawing conclusions on dominant ENSO mechanisms from just one or two models is not sufficient. Several model studies also have shown that 200 to 300 years of data are needed to robustly assess significant changes in ENSO properties, at least in GCMs (Wittenberg, 2009; Stevenson et al., 2010; Collins et al., 2019; Magnan et al., 2019), but also most likely in observations.

9.3.1. Process Understanding

Reviewing studies that used coupled models to understand ENSO processes would be both lengthy and a duplication of many parts of this monograph. Here we review how GCMs help to understand ENSO, provide a few examples, and discuss their advantages and limitations.

Systematic errors in ENSO properties, documented in successive CMIP generations (Delecluse et al., 1998; van Oldenborgh et al., 2005; Capotondi et al., 2006; Guilyardi, 2006; AchutaRao and Sperber 2006; Bellenger et al., 2014; C. Chen et al., 2017), have been traced back to a number of mechanisms, helping to identify their key role. For example, earlier CMIP generations (Delecluse et al., 1998) with coarse ocean grids confirmed the importance of ocean equatorial waves for ENSO dynamics. More recently, CMIP3 and CMIP5 highlighted the importance of correctly representing atmospheric deep convection, trade wind strength, and cloud feedbacks (Lloyd et al., 2012, Bellenger et al., 2014, Dommenget & Yu, 2016). As some of these errors have gradually been reduced in more recent versions of the models, remaining biases have also traced to other processes (e.g., atmospheric intraseasonal variability or oceanic vertical mixing, see section 9.5), which helps identify them as secondary processes for ENSO. However, error compensation between large biases may inhibit the understanding of major processes in the real system (Guilyardi et al., 2004; Bellenger et al., 2014; Figure 9.1). These can only be seen once these major biases disappear. For example, the impact of ocean resolution on ENSO properties (beyond that of resolving equatorial waves, which was achieved at the end of the TOGA period) could only be shown once the atmosphere resolution was high enough (Roberts et al., 2009, Haarsma et al., 2016).

Early theoretical models and EMICs of ENSO were devised as "anomaly models." At the same time, early coupled GCMs had to resort to flux corrections to avoid large mean state drift. This combination of factors hid for many years the fact that ENSO interacts with both the mean state and annual cycle. Systematic analyses of CMIP3, the first generation of models that (mostly) did not use flux correction, showed that ENSO properties and errors could be linked to mean state errors (e.g., Wittenberg, 2002; Guilyardi, 2006; Taschetto et al., 2014; Graham et al., 2017). For example, several studies showed an inverse relationship between the strength of the annual cycle in the east Pacific and the amplitude of ENSO (Guilyardi, 2006; Fedorov & Philander, 2000). Recent theoretical work has also explored this issue and the mechanisms involved, and it is now an active field of research (cf. chapter 8), largely relying on models. As an example, the nonlinear interaction between ENSO and the annual cycle is able to generate timescales arising from combinations of the annual and ENSO frequencies and provides a source of irregularity (Stuecker et al., 2013, 2017; Ren et al., 2016). This can help trace back errors in ENSO properties to errors in the annual cycle, a notoriously difficult feature to model correctly in CGCMs, especially in the east Pacific where the double

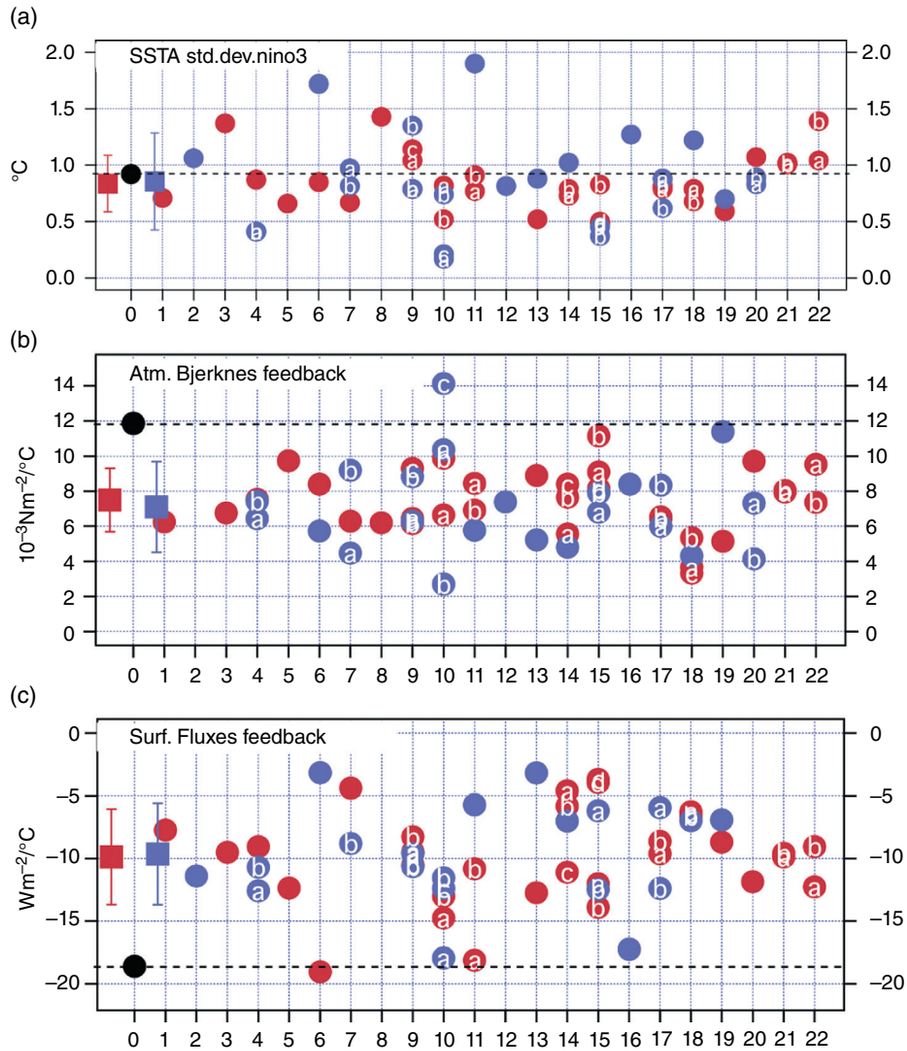

Figure 9.1 Process-based evaluation of ENSO in coupled models (see section 9.4) is now a standard strategy to understand if ENSO properties are simulated correctly via the right balance of processes. For example, Bellenger et al. (2014) have shown that CMIP models achieved the right ENSO amplitude (panel a) as a compensation between too-weak Bjerknes positive feedback (panel b) and too-weak negative surface heat flux feedback (panel c). Numbers on *x*-axis are CMIP models (blue is CMIP3 and red is CMIP5, letters refer to different models within the same generation). Squares indicates multimodel mean. Black circle and dashed line indicate observations. See Figure 1 of Bellenger et al. (2014) for further details.

Intertropical Convergence Zone (ITCZ) systematic error is often associated with the spurious semiannual cycle.

The diversity of ENSO representations in the first generation of models without flux corrections (CMIP3) was unexpected. A debate was begun over the reasons why, and soon two families of arguments emerged: (i) either this diversity was spurious and due to model errors, or (ii) the simple balance of processes proposed by ENSO theories was actually more complex. The debate was resolved by recognizing that both views were partly correct. An example of the above discussion is the debate about the role of the atmosphere in setting ENSO properties, which started in the late 1990s. Studies using a mix of various AGCMs and OGCMs showed that the AGCM had a dominant role in setting ENSO properties (and errors) in GCMs (Guilyardi et al., 2004). This was unexpected as ENSO, due to its slow timescale, was then mostly viewed as primarily involving oceanic processes (Neelin et al., 1998). Atmospheric processes in ENSO theories were then (and in some sense still are) represented by a mostly steady-state response to surface heating (Gill, 1980), forming the atmospheric branch of the Bjerknes feedback, and a local and linear Newtonian damping associated with surface fluxes. Detailed analysis

of model simulations, as well as better observations of the tropical atmosphere, have since helped revisit the role of the atmosphere in ENSO. Heat flux feedbacks, linked with clouds, convection, and boundary-layer physics, were shown to play a central role in ENSO (Guilyardi et al., 2009), and together with the Bjerknes feedback exhibit marked nonlinearities, like those associated with the convective threshold (Lloyd et al., 2012; Bellenger et al., 2014; Takahashi & Dewitte, 2016).

Models also offer a unique framework to make closed budget computations, unlike observations, which have insufficient sampling both in space and in time. This helps clarify the relative balance of mechanisms in the ocean during ENSO (Vialard et al., 2001; Ray et al., 2018b) or develop integral energetics approaches (Brown & Fedorov, 2010; Brown et al., 2011).

Since the 1997–1998 large El Niño event, the role of atmospheric intraseasonal variability (ISV), namely WWBs, has been investigated in increasing detail. Again, due to limited observations, models have been choice tools to investigate this new field (see review by Lengaigne et al., 2004). Beyond exploring mechanisms, models can be used to increase the sampling and explore the ENSO/ISV relationship more robustly than in the limited observational record (Puy et al., 2017; Chiodi & Harrison, 2017; Larson & Kirtman, 2015). Another benefit is the ability to decouple the respective roles of the ocean and the atmosphere to infer causality in an otherwise strongly coupled and highly variable system (van Oldenborgh, 2000; Vecchi et al., 2006; Gebbie et al., 2007; Hu & Fedorov, 2016; Puy et al., 2017). For instance, the same WWB can be applied at regular time intervals to an interannually varying simulation (Puy et al., 2017; Figure 9.2) to assess the role of the ISV forcing on ENSO development and strength. One remaining limitation to this day is of course the model's ability to generate both correct ENSO behavior and correct ISV variability characteristics, which remains a challenge (Hung et al., 2013; Ahn et al., 2017).

To explore the predictive power of the subsurface heat recharge in the ocean, Larson and Kirtman (2015) used an approach in which any interannual precursors were coherently removed in the tropical Pacific, thereby isolating the role of high frequency noise (WWBs) in ENSO predictability. They showed that, without prior heat recharge, the occurrence of WWBs in March could precondition the Pacific towards an El Niño event later in the year, whereas the other months were less sensitive. Using a multimodel approach, in which a selection of CMIP5 models that correctly simulate ENSO properties is made, Planton et al. (2018) found an El Niño/La Niña asymmetry in the predictive power of the heat recharge, with discharge being a more reliable predictor of La Niña occurrence and amplitude than recharge is for El Niño.

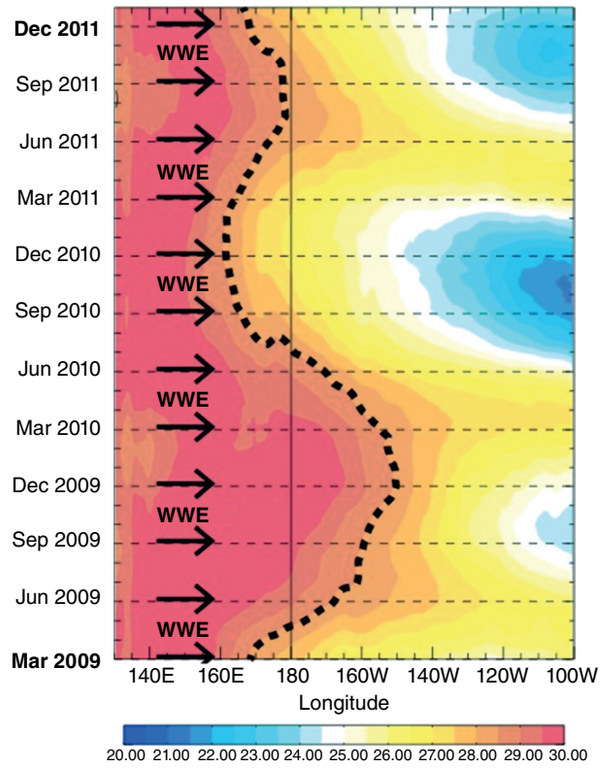

Figure 9.2 A set of experiment where the same WWB (a.k.a. WWE) is applied at different seasons and interannual conditions. An intraseasonally filtered forcing and an idealized WWB are used. This strategy allows a clear separation of causes and effects of the impact of WWB on ENSO and, in particular, the description of the role of the stochastic part of WWBs, i.e. the component of the WWBs not responding to the background conditions. Shading is SST with the dashed line representing the 28.5C isotherm, i.e. the eastern edge of the warm pool (see Puy et al., 2016).

In a related study, Neske & McGregor (2018) used a forced OGCM to distinguish the slow, dynamically driven recharge (e.g. Izumo et al., 2018) from the instantaneous, ISV-driven recharge and showed that the relative importance of the two sources depended on the ENSO state.

ENSO events display a broad spectrum of spatial structures, ranging from very strong events with the largest SSTA in the eastern Pacific (EP events) to weaker events that peak in the central Pacific (CP events). This diversity of spatial patterns has received considerable attention in recent decades (Capotondi et al., 2015b, and references therein; see also chapter 4) due to the increased occurrence of CP events after the year 2000, and to the recognition that atmospheric teleconnections are sensitive to the location of SST anomalies in the equatorial Pacific. Event-to-event differences also include time evolution, direction of propagation, event asymmetries, etc.: a range of aspects that has recently been termed "ENSO

complexity" by Timmerman et al. (2018). Due to model biases such as the equatorial cold tongue (ECT) bias, many models have difficulty in simulating a diversity of spatial patterns, as discussed in chapter 4. However, some models do exhibit some degree of realism in simulating ENSO diversity, including the continuum between CP and EP cases. These models have been invaluable for gaining insight into the nature and leading dynamical feedbacks of different types of El Niño events, with a much higher degree of statistical significance than can be achieved using the shorter observational record (Kug et al., 2010, Capotondi, 2013).

Multicentury preindustrial climate model simulations have also shown the possibility of a low-frequency modulation of ENSO diversity, with decadal epochs dominated by either EP or CP event types that can occur even in the absence of any external forcing (Kug et al., 2010; J. Choi et al., 2011; J. Choi et al., 2012; Wittenberg et al., 2014). The possibility of these intrinsic decadal variations, which as yet would be difficult to determine from short observational records in the presence of past natural and anthropogenic radiative forcings, suggests caution in interpreting recent changes in ENSO character (e.g. the larger number of CP events during the first decade of the 21st century) as trends associated with global warming (Yeh et al., 2009; Newman et al., 2018). While global warming can be expected to influence ENSO diversity, the nature of this influence is still unclear (e.g., Cai et al., 2018; chapter 13). A better understanding of the reliability of model projections will be critical to clarify this point.

Sensitivity experiments can help make progress on questions even less constrained by observations, a limitation made even more acute because of ENSO diversity. For example, the specific role of ENSO in tropical Pacific decadal variability is explored in simulations in which either the tropics or the midlatitudes are constrained, to either climatology or to a fixed interannual cycle for all surface coupling fields or just a subset (Liu & Di Lorenzo, 2018). The role of other basins can also be explored using partially coupled simulations to disentangle what is driving ENSO from what is driven by ENSO (Kajtar et al., 2017, Terray et al., 2015). The inherent limit of these studies is the lack of reliable observations for the many decades needed to validate the model behavior and ensure the robustness of the relationships exhibited.

9.3.2. Response to External Forcing

Changes in ENSO behavior induced by external forcing (e.g. solar, volcanic, greenhouse gases) can arise from changes in the mean state or from impacts on specific ENSO feedbacks (Collins et al., 2010; Vecchi & Wittenberg, 2010; Flato et al., 2013). Again, because of the lack of data in the past, models are key to explore these relationships (see chapters 5, 12, and 13). As described above and in other parts of this monograph, the mean state and decadal-to-multidecadal variability strongly influence ENSO behavior. One can use external forcing to distinguish what is the mean climate (e.g., no variations of external forcing, even if only theoretical) and what is slow variability (e.g., driven by changes in external forcing). In a multicentury preindustrial simulation (or any simulation in which external forcing is kept constant), and in the absence of serious model drift, the mean can indeed be viewed as fixed, and any other variation can be interpreted as internal variability (e.g. Wittenberg, 2009; Wittenberg et al., 2014). Distinguishing the mean from the variability gets more complicated when the external forcing varies with time (e.g. volcanic eruptions and greenhouse gases), due to the multicentury statistics or large ensembles needed to assess robust changes (Stevenson et al., 2010; Predybaylo et al., 2017). Alternative definitions of the mean can help to disentangle the associated intricacy. For example, Khodri et al. (2017) have shown that using the relative SSTA, i.e. the SSTA computed by removing the tropical Pacific spatial mean, could clarify the impact of volcanic eruptions on ENSO by focusing on the gradients, helping to reconcile previous studies (Figure 9.3).

Here again, the multimodel coordinated approach (or the use of large ensembles) helps by increasing the signal to noise ratio, making it easier to robustly attribute changes in ENSO to changes in external forcing (Figure 9.3). This is not systematic, as small ensembles with large model errors can lead to unclear responses (Zheng et al., 2008).

Coordinated simulations as defined in CMIP (Eyring et al., 2016) explore different external forcing conditions such as paleo (paleoclimate MIP: PMIP; Kageyama et al., 2016), historical change and the impact of different forcings (detection and attribution MIP: DAMIP; Gillett et al., 2016) or future projections (scenarioMIP; O'Neill et al., 2016). Common protocols are defined and forcing fields are provided to modeling groups for solar, volcanic, greenhouse gas, and land surface use (see https://explore.es-doc.org/). The way models conform to protocols varies and is now carefully documented, as this may affect the interpretation of results and/or differences among model responses.

How well internal variability is simulated directly impacts the ability of models to respond correctly to external forcings. For example, if the simulated variability is stronger than observed, the forced signal may take longer to emerge from the corresponding "noise" of internal variability. Conversely, a model with too little variability can appear as either too sensitive to external forcing or not sensitive enough if the mechanisms that drive the response are the same as those that drive variability. The research community is therefore working to assess the fitness for purpose of models to study the ENSO response

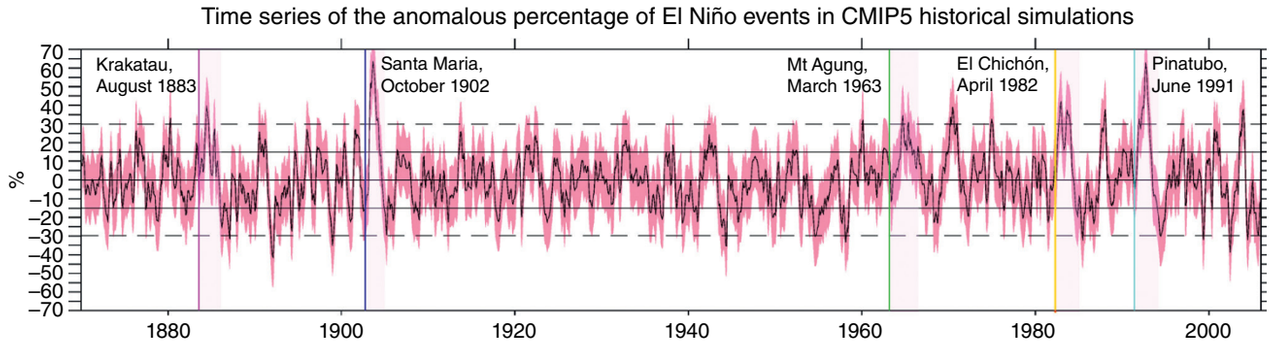

Figure 9.3 Anomalous percentage of CMIP5 historical simulation members with an El Niño occurrence for the entire historical period (136 years). The anomalous percentage is given relative to the climatological rate over the entire period. El Niño events are defined as Niño3.4 positive relative SSTAs exceeding 1/2 standard deviation. The vertical colored lines localize each eruption date and the pink shading a period of 2 years following the eruption. Continuous and dashed horizontal lines indicate one and two standard deviations respectively. The red shading outlines one standard deviation from the mean of the ensemble (Khodri et al., 2017).

to changing climate (Flato et al., 2013, and section 9.4). Previous studies have shown that the atmospheric response to ENSO is not a good analog of the atmospheric response to future climate warming, e.g. ENSO sensitivity is not a proxy of climate sensitivity (Bony et al., 1997), even though some of the same mechanisms play a part (e.g. changes in atmosphere deep convection and clouds). A recent study that explored the links between internal variability in CMIP models and their response to external forcings showed that models in which clouds more strongly amplify ENSO-induced surface temperature changes also tend to be the models that are more sensitive to external forcings (Lutsko & Takahashi, 2018).

9.4. EVALUATING ENSO IN MODELS

In this section we review how ENSO is evaluated in coupled GCMs. We then discuss some common model biases and their suspected sources.

9.4.1. Diagnosing Model Biases

As described in the preceding chapters and Timmermann et al. (2018), ENSO involves complex interactions across a vast range of space and time scales. This poses major challenges for simulating ENSO and for diagnosing the sources of bias in ENSO simulations. The theoretical foundations in chapters 6–8 provide a framework for understanding ENSO and have motivated diagnostics that are now used to evaluate and intercompare ENSO simulations.

Although ENSO is mainly a seasonal-to-interannual phenomenon driven by air-sea interactions in the tropical Pacific, it also interacts with the extra tropics and other ocean basins (chapters 11, 14, and 15) and involves timescales ranging from subdiurnal (atmospheric convection, the diurnal cycle, and mixed layer processes) to decadal to centennial (chapters 5 and 8). ENSO further depends on small-scale processes (e.g. convection and cloud physics in the atmosphere, and eddy-induced mixing in the ocean) that require short time steps and fine model grids, as well as careful parameterizations of subgrid scale processes. Capturing this wide range of scales can require multicentury simulations with powerful supercomputers, saving high-frequency and high-resolution diagnostics that result in enormous model datasets. The challenge is making sense of that mountain of data and drawing conclusions about the model's reliability for forecasts and projections.

ENSO's diverse scales and interactions also pose challenges for the observing system, by requiring a combination of dense high-frequency global coverage and continuous monitoring over many decades (chapters 3 and 5). At present, the existing observational records and reanalysis products remain imperfect targets for model development due to short records, instrumental errors, evolving observing methods and networks, and misrepresentation by reanalyses of the variables, regimes, and scales actually observed. As models continue to improve, reconciling the remaining biases and disparities among observational products becomes even more important. Further progress will require longer, more detailed, more reliable, and more representative observations and reanalyses, along with new field studies to underpin improved model parameterizations.

Intrinsic modulation of ENSO on interdecadal timescales (chapter 8) implies that multicentury records and/or large ensembles are needed to evaluate and intercompare ENSO simulations and to assess changes in ENSO arising from external forcings. Indeed, the instrumental

record may not yet be long enough to fully constrain ENSO simulations, especially for the amplitude, spectrum, and diversity of ENSO (e.g. Wittenberg, 2009; Wittenberg et al., 2014; Newman et al., 2018). Thus, complementary methods to evaluate ENSO simulations have recently included paleo constraints (chapter 5) as well as process-based diagnostics and statistical emulators (Newman et al., 2011, 2018; C. Chen et al., 2017; Ding et al., 2018) that can be used to infer long-term ENSO behavior from relatively short observational records.

Comparing multiple models can establish which biases are widespread among models and which biases are idiosyncratic. Intercomparisons can also identify particular resolutions, parameterizations, or climatological biases as likely sources of ENSO biases. An example is shown in Figure 9.4, which illustrates the diversity of Pacific ECT intensities and ENSO amplitudes simulated by the CMIP5 models, in the context of intrinsically generated variability and radiatively forced changes. For the time-mean SST, most of the CMIP5 models simulate colder ECTs than observed over the historical period (vertical black line), and all show a warming of the ECT in the 21st century (blue triangles) that far exceeds the range expected from intrinsic variability alone (horizontal gray bars). There is no clear relation among the CMIP5 models between the strength of the 20th-century ECT SST bias and the magnitude of future ECT warming. For the ENSO SSTA amplitude, the models show a wide range of simulated amplitudes, with some stronger and others weaker than observed over the 20th century. Moving to the 21st century, most models show a weakening of ENSO in the 21st century, but the models that show strengthening of ENSO tend to do so more significantly relative to their preindustrial control runs. There is no clear relation between the simulated 20th-century ENSO amplitude and the projected amplification or attenuation of ENSO in the 21st century. The diverse set of models also provides an ensemble of opportunities to investigate how ENSO biases and sensitivities depend on ENSO feedbacks or the background climate state, providing "emergent constraints," as discussed in section 9.4.3.

An essential first step in evaluating ENSO is to understand the climatological context in which it evolves – namely the background time-mean state and seasonal cycle, as these play a key role in many ENSO mechanisms. In examining the tropical Pacific diagnostics, particular attention must be paid to (i) east-west and north-south SST contrasts, (ii) the meridional asymmetry of SST and rainfall, (iii) the surface zonal wind stress (τ^x) over the equatorial waveguide, (iv) the meridional wind stress (τ^y) in the southeast Pacific, and (v) the off-equatorial wind stress curl. Below the ocean surface, key climatological diagnostics include (i) the isothermal layer depth, which helps determine the sensitivity of SST to surface heat fluxes; (ii) the equatorial thermocline depth, slope, intensity, and sharpness; (iii) the equatorial undercurrent and South Equatorial Current; and (iv) the equatorial upwelling, as well as (v) the components of the surface mixed layer heat budget near the equator.

Numerous diagnostics are used to assess the structure, evolution, mechanisms, and impacts of ENSO. For spatial structure, monthly means are used to create maps of amplitude (standard deviation), nonlinearity (e.g. skewness), and various responses/feedbacks (e.g. based on correlations, regressions, or composites either using an ENSO index like Niño-3 SSTA, or using local SSTA). Composites can be used to highlight nonlinear features and can also be easily conditioned on the seasonal cycle. Lag-regressions or lag-composites onto ENSO indices are useful for identifying seasonal modulation and zonal/meridional propagation, which is often seen for equatorial SSTA and τ^x. To characterize the temporal variability of ENSO (e.g. period, interdecadal amplitude/frequency modulation, duration, and interevent spacing), various diagnostics are used, including lag-autocorrelations, spectra, and wavelet analyses of ENSO indices. The simplified statistical and dynamical methods described in section 9.2 can also serve as powerful diagnostics, by fitting them to observations and coupled models and then comparing the fitted parameters. This can highlight key differences in feedback mechanisms, stochastic forcings, growth rates, predictability, long-term modulation, and sensitivities to parameter and forcing changes (e.g. Kim & Jin, 2011; Atwood et al., 2017; Capotondi et al., 2018).

In addition to the diagnostics outlined above, numerous approaches have been used to isolate and understand the sources of model biases. One approach is to limit the potential sources of bias by isolating particular model components and driving them with observations, such as the classical atmosphere-only MIP (AMIP) and ocean-only MIP (OMIP) simulations (a.k.a. "forced simulations"). Besides helping to identify the sources of model biases, isolating a model component enables direct event-by-event comparisons with observations and allows smaller ensembles, since the imposed synchronization eliminates most of the basin-scale intrinsically generated variability. In the past, modeling centers often developed model components in isolation, only coupling them near the end of the development cycle. However, experience showed that this was often unsuccessful, leading to large drifts in the coupled configuration. Now many centers couple early and often in the development cycle, which helps to maintain a focus on the parts of the simulation essential for successful coupling over the tropical Pacific region, namely, the surface fluxes simulated by the atmosphere

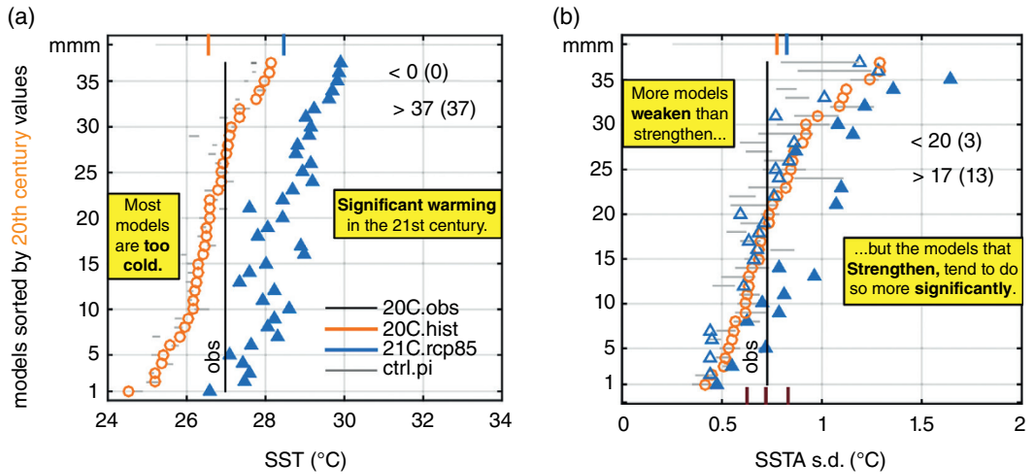

Figure 9.4 Values simulated by the CMIP5 models for (a) climatological mean SST (°C) averaged over the Niño-3.4 region (170°W–120°W, 5°S–5°N), and (b) standard deviation of SSTAs (°C) averaged over the Niño-3.4 region. Simulations correspond to 20th-century historical forcings (1900–1999, orange circles), the 21st-century RCP8.5 scenario (2000–2099, blue triangles), and the central 95% range for 100-year running statistics from the preindustrial control run (horizontal gray bars). Black vertical line indicates the observed value for 1900–1999 computed from the HadISST.v1.1 reconstruction. The multimodel mean (MMM) values for the orange and blue symbols are indicated with similarly colored vertical bars along the top abscissa. 21st-century values that exceed the 20th century are shown with filled blue triangles, and their count is indicated by the > label (with the number of significant changes relative to the gray bars indicated in parentheses). Twenty-first-century values that fall below the 20th century are shown with hollow blue triangles, and their count is indicated by the < label (with the number of significant changes in parentheses). Brown vertical bars on the bottom abscissa indicate the (2.5, 50, 97.5) percentiles from a 4000-year simulation of a statistical model fit to the HadISST.v1.1 observation. The models are sorted in the vertical according to the 20th-century values (orange circles). Adapted from Figure 9 of C. Chen et al. (2017).

and the surface mixed layer and SST simulated by the ocean. The AMIP and OMIP frameworks remain very helpful tools, however, for isolating biases identified in coupled models.

Another strategy is to only partially enable the coupling, by nudging or overriding one of the variables involved in the exchange. For example, the simulated SST can be nudged (restored) with a short time scale (e.g. 5 days) toward observed time-varying SSTs, to test the performance of the atmosphere and ocean simulations in the presence of both high-frequency (diurnal) coupling and close-to-observed SST variability (Kamenkovich & Sarachik, 2004; Zhu & Kumar, 2018; Vecchi et al., 2019). Ocean biases that develop in the nudged context but not in the OMIP context can indicate a problem, for example, with the simulation of the wind stress by the atmosphere component. The nudging term also provides a valuable diagnostic, indicating the degree of correction required to keep the SST close to those observed in different locations and dynamical conditions. This approach can also be applied regionally, to further isolate the sources of model bias (Large & Danabasoglu, 2006; Small et al., 2015; Song & Zhang, 2016; McGregor et al., 2018).

Another valuable technique is to compute a climatology of the nudging term and wind stress biases from the nudged run described above. A new coupled run can then be performed in which the nudging is turned off, but now the seasonally varying (but interannually constant) nudging climatology is prescribed. This technique and its variants, known as "flux adjustment" or "flux correction," help to maintain the climatology of the coupled model close to observations, without restricting the development of anomalies relative to that climatology. This framework can help diagnose how biases in simulated ENSO dynamics are related to a model's climatological biases (Magnusson et al., 2013a; Ray et al., 2018b). Several studies have shown that flux adjustment can improve a model's simulated tropical Pacific climatology, seasonal cycle, ENSO, and seasonal forecast skill (Manganello & Huang, 2009; Kröger & Kucharski, 2011; Magnusson et al., 2013a, 2013b), although results especially for forecast skill appear to be model dependent (Spencer et al., 2007; Pan et al., 2011).

The ability of a model to reconstruct and forecast either real-world ENSO events or its own events can be used to assess the degree of ENSO's long-term memory and predictability (Wittenberg et al., 2014; Karamperidou

et al., 2014; Ding et al., 2018, 2019). Ding et al. (2018) found that some models are now realistic enough that their unforced control runs contain close "model-analogs" of real-world conditions, and the evolution of those analog trajectories can actually provide useful ensemble forecasts of the real world, with skill approaching that of state-of-the-art assimilation and forecast systems. The ability of a model's analogs to reconstruct and forecast real-world ENSO conditions is thus a potentially powerful diagnostic of model performance, assessing both the shape of the model's attractor and the evolution of its trajectories on that attractor.

Data assimilation can assist in diagnosing model biases, through the analysis of the increments needed to adjust the model solution toward observations. A systematic increment structure can help to localize persistent dynamical biases in the model. The performance of model forecasts of the real world, initialized via data assimilation, can also provide valuable information about model biases. If the assimilated state lies far from the model attractor, this can induce an "initialization shock," which rings through the model's climate system and reduces forecast skill. Once the model is released from data assimilation and run in forecast mode, the location and time scale of bias development can help to isolate biases in particular processes (Vannière et al., 2014). For example, a bias that appears within a single day would have to involve local biases in clouds, surface heat fluxes, or mixed layer dynamics but would rule out remotely forced internal waves in the ocean. Using this approach, it has been shown that a single bias (e.g. the ECT error described below) can have model-dependent sources (Vannière et al., 2013).

9.4.2. Key Model Biases

A number of common ENSO biases have been identified in CGCM simulations, some persisting since earlier model intercomparisons (Guilyardi, 2006, Guilyardi et al., 2009, 2012a, 2012b; Bellenger et al., 2014, Capotondi et al., 2015a; Santoso et al., 2019). Here we discuss those biases and how they are related to biases in the simulated background climatology.

9.4.2.1. Biases in the Background Climatology

Common biases in the CGCM-simulated background climatology include

1. An overly strong ECT that extends too far west, associated with a cold SST bias in the equatorial Pacific.
2. A warm SST bias near the coast of South America.
3. An equatorial Pacific dry bias, associated with the excessive ECT.
4. An excessive "double" ITCZ south of the equator in the east Pacific (J. Lin, 2007).
5. A southern Pacific convergence zone (SPCZ) that is too zonally oriented.
6. An overly intense hydrologic cycle over the tropical Pacific, with excessive evaporation and rainfall (de Szoeke & Xie, 2008; Wittenberg et al., 2018).
7. Biases in the cloud regimes over the eastern and central Pacific (Lloyd et al., 2009, Sun et al., 2009, Bellenger et al., 2014).
8. Equatorial τ^x that is too strong or too weak, which then affects equatorial upwelling and the zonal tilt of the equatorial thermocline.
9. Overly cyclonic wind stress off-equator, associated with a too-rapid poleward intensification of τ^x. This can lead to excessive Ekman suction and poleward Sverdrup transport off-equator, shoaling the equatorial thermocline and contributing to an ECT cold bias (Wittenberg et al., 2018).
10. Biases in the equatorial thermocline depth, intensity, sharpness, and zonal slope.

These biases can be masked by other deficiencies in the model via error compensation (Guilyardi et al., 2004, 2009; Wittenberg et al., 2018; Ray et al., 2018a, 2018b; Vijayeta & Dommenget, 2018). For example, many processes can influence the structure and maintenance of the ECT, including vertical mixing in the upper ocean off-equator (Anderson et al., 2009), subtropical cloud albedos (Burls et al., 2014), excessive equatorial zonal wind stress (Vannière et al., 2013), temperature biases subducted in the subtropics (Thomas & Fedorov, 2017), errors in the subtropical wind stress that controls the strength and structure of the shallow meridional overturning subtropical-tropical cells and equatorial upwelling (McPhaden & Zhang, 2002; Capotondi et al., 2005), and SST biases in the tropical Indian and Atlantic oceans (Kajtar et al., 2017). This diversity of possible mechanisms is a key reason that it remains a challenge to correctly simulate the ECT in GCMs.

Climatological biases can affect ENSO feedbacks and sensitivities by displacing climatological features, and their associated ENSO variability, away from their observed locations. Background biases also affect the intensities and spatiotemporal phases of the leading terms in the mixed layer heat budget, namely, the heat flux damping, thermocline feedback, zonal advective feedback, and Ekman feedback, which then induce biases in ENSO properties (An & Wang 2000; Wittenberg 2002; Kim & Jin, 2011; Graham et al., 2017).

9.4.2.2. Biases in ENSO

As described in recent reviews (Guilyardi, 2006; Guilyardi et al., 2009, 2012a, 2012b; Bellenger et al., 2014; Capotondi et al., 2015a; Santoso et al., 2019), common ENSO biases in CGCMs include

1. Amplitude errors, which can also affect the skewness, diversity, and interdecadal modulation of ENSO

and the ability of ENSO to affect the multidecadal-mean climate.

2. Errors in spectrum, including the dominant ENSO period and irregularity. In many models the ENSO spectrum is too sharply peaked, and the ENSO period is too regular and biennial.

3. Too little synchronization of ENSO to the annual cycle, or a synchronization of ENSO to the wrong season. This can result from problems simulating the climatological seasonal cycle of the ITCZs (Wittenberg et al., 2006; Abellán et al., 2017), the SST-cloud and thermocline-SST feedbacks of ENSO (Rashid & Hirst, 2016), and the seasonally mediated impacts of ENSO on remote regions (Lee et al., 2016, 2018; W. Zhang et al., 2016).

4. Errors in the level of interdecadal modulation of ENSO behavior.

5. SSTA patterns that are displaced too far west, disconnected from the South American coast, too symmetric about the equator, and show too little interevent diversity in peak longitude (Capotondi et al., 2015a; chapter 4, this volume).

6. Atmospheric response patterns of rainfall and teleconnections that are displaced too far west.

7. Too little skewness of ECT SSTAs toward warm events (An et al., 2005; Dommenget et al., 2013; T. Zhang & Sun 2014; C. Chen et al., 2017), and too little skewness of central equatorial Pacific τ^x toward westerly anomalies (K.-Y. Choi et al., 2013).

8. Equatorial τ^x anomalies that are too weak, too far west, and too narrow in the meridional direction (Guilyardi, 2006). This can affect ENSO amplitude via a reduced zonal wind feedback (Figure 9.1) and can accelerate the oceanic adjustment to wind anomalies and shorten the ENSO period (Capotondi et al., 2006)

9. Too little damping of SSTAs by surface heat fluxes, often due to a weak cloud shading response associated with biases in cloud regimes, and other mean state biases (Lloyd et al., 2012, Bellenger et al., 2014, Dommenget & Yu, 2016).

10. Insufficient cross-timescale linkage between ENSO, its intraseasonal precursors, and Pacific decadal modes (Di Lorenzo et al., 2015; Newman et al., 2016; Wang & Miao, 2018; Liguori & Di Lorenzo, 2018; R. Lin et al., 2018). These errors appear to be linked in part to the magnitude of the climatological ECT cold SST bias (Lyu et al., 2015).

Many of these errors in ENSO simulations can be linked to biases in the background climatology. Atmospheric convection and rainfall patterns over the tropical Pacific are sensitive to the relative temperature difference between the local SST and the tropical-mean SST, especially over the warm pool (He et al., 2018). Thus, models with excessively cold ECTs and a westward-displaced warm pool tend to have westward-displaced ENSO patterns (e.g. Wittenberg et al., 2006; Ham & Kug, 2015). This is often associated with a modified distribution of convective and subsidence regimes, leading to deficient atmosphere feedbacks in the east and central Pacific (Lloyd et al., 2012, Bellenger et al., 2014) and overamplified or overdamped ENSO events. Such biases in the background state can even lead to unrealistic double-peaked El Niños (Graham et al., 2017), due to the zonal-advective feedbacks at the warm pool's eastern edge being displaced too far west of the thermocline feedbacks occurring further east. Westward displacement of ENSO's SSTAs can also weaken the interevent diversity of SSTA patterns, as it becomes more difficult to generate SSTAs in the eastern ECT that induce a τ^x response with sufficient zonal fetch to produce strong thermocline feedbacks (Ham & Kug, 2012; Kug et al., 2012). Improper balances between zonal and thermocline feedbacks can also affect the zonal propagation direction of SSTAs (Ham & Kug, 2015; C. Chen et al., 2017). A model with a poleward-displaced ITCZ and SPCZ can also show reduced nonlinearity of the equatorial τ^x response to SSTAs, which then affects ENSO's warm-cold asymmetries of amplitude, duration, and transition (K.-Y. Choi et al., 2013, 2015).

As described above for biases in the background state, biases in ENSO can mask each other. For example, a model with both a weak equatorial τ^x response (which tends to weaken ENSO) and weak surface heat flux damping (which tends to strengthen ENSO) can exhibit a reasonable ENSO amplitude for the wrong reasons (Guilyardi et al., 2009; Vijayeta & Dommenget, 2018). Similarly, a model with a climatological cold SST bias in the ECT may still be able to produce realistic atmospheric responses during the El Niño phase, if it also has excessive warm SSTAs to flatten the zonal and meridional SST gradients across the tropical Pacific, thereby favoring atmospheric convection in the central and eastern equatorial Pacific.

Errors in ENSO amplitude can also affect the multidecadal-mean climate, via nonlinearity and temporal blurring of the seasonal-to-interannual motions of features like the ITCZs, warm pool edge, and thermocline (Watanabe & Wittenberg, 2012; Watanabe et al., 2012; Ogata et al., 2013; J. Choi et al., 2013; Atwood et al., 2017).

9.4.2.3. ENSO Response to External Forcings

As described in chapter 13, GCMs produce diverse and nonmonotonic projected responses of ENSO to future changes in radiative forcings (Vecchi & Wittenberg, 2010; Collins et al., 2010; C. Chen et al., 2017, Rashid et al., 2016). Depending on the model, the future amplitude of ENSO SSTAs can increase, decrease, or show no significant change, with no clear link to the magnitude of the time-mean ECT SST bias in the historical simulation (C. Chen et al., 2017).

Uncertainties in ENSO's future SSTA amplitude arise from competing changes in ENSO's intense air-sea feedbacks, which amplify the sensitivity of ENSO (and its future response) to biases in the models (Collins et al., 2010; DiNezio et al., 2012). Studies have shown that the sensitivity of the background state and ENSO SSTAs to future anthropogenic forcings depends strongly on the present-day simulated spatial structure of key climate regimes, including the regions of intense convection, cloudiness, and evaporation (Xie et al., 2010), the intensity of the ECT (Huang & Ying, 2015), the strength of convective cloud shading response to SSTAs (Ying & Huang, 2016a), the intensity of equatorial Pacific upwelling (Ying & Huang, 2016b), and the future warming of the tropical Indian and Atlantic oceans relative to the tropical Pacific (Luo et al., 2012; Wieners et al., 2017). Model biases in these climatological features can therefore lead to biases in the sensitivity of ENSO to future change, reducing confidence in future projections.

There is also substantial intrinsic modulation of ENSO that is unrelated to external forcings (Wittenberg, 2009, 2015; Stevenson et al., 2010), which can mask forcing-induced changes in short observational records. For example, Newman et al. (2018) examined 30-member historical ensembles from the NCAR-CESM-LE and GFDL-FLOR-FA CGCMs, and found that while both ensembles simulated a slight trend toward stronger ENSO SSTAs over the past century, those trends were of the same magnitude as the intrinsic modulation of ENSO among realizations with the length of the observational record. This suggests that the forced component of change, even if it were as large in reality as in the models, would be difficult to detect in the single century–long realization yet available from the historical observations. Consistent with this, Newman et al. (2018) found that the observed trend in ENSO SSTA amplitude (the strength of which differed depending on the historical SST reconstruction used) did not exceed the range expected for a null hypothesis of stationary ENSO dynamics, estimated using a stochastically forced linear inverse model tuned to the historical observations.

It has also been suggested that models may systematically underestimate intrinsic decadal variations in the tropical Pacific (Kociuba & Power, 2015), for instance, due to reduced SSTA persistence and/or reduced inter-basin connections associated with model SST biases in the tropical Atlantic (McGregor et al., 2018). Reduced decadal variability might then affect the models' ability to capture a realistic range of intrinsic ENSO modulation.

Despite the uncertainties mentioned above, there are aspects of future ENSO change that are relatively robust among the model projections (chapter 13), including a tendency for ENSO rainfall variations over the tropical Pacific to increase and shift eastward and equatorward as the tropical atmosphere moistens, especially during El Niño (Power et al., 2013, 2017; Cai et al., 2014; Huang & Chen, 2017), and a tendency for more eastward propagation of ENSO equatorial SSTAs in the future (C. Chen et al., 2017). However, intermodel consensus does not necessarily mean that the projections are correct, as many models have similar climate biases that could affect their sensitivities to future change. In particular, there is concern that the inability of most models to capture the recent observed decadal strengthening of the Walker circulation (Power et al., 2017) may indicate that they either underestimate the intrinsic decadal variability or overestimate the externally forced warming of the eastern equatorial Pacific, thereby reducing the east-west SST gradient.

9.4.3. Emergent Constraints for Future Changes in ENSO

A potentially powerful approach to deal with the above uncertainties is to examine how model projections depend on model biases. If robust relationships can be found, then it may be possible to extrapolate the expected sensitivities of the real world from the diverse model results, providing "emergent constraints" for the real-world response (e.g. Heinze et al., 2019).

An example is shown in Figure 9.5 adapted from Ham & Kug (2015), which indicates that among the CMIP5 models there is a relationship between the ECT intensity and the longitudinal location of the ENSO anomaly patterns. Models with weaker/better ECTs tend to show an ENSO response closer to observed, with patterns of rainfall, wind stress, and SSTAs that shift farther eastward and equatorward during El Niño. By extending such relationships to include the observations, estimates can be made regarding the real-world sensitivities, essentially leveraging the intermodel diversity to provide emergent constraints for the sensitivities based on a large set of models.

A second example is that among the CMIP3 models that produced a reasonably realistic ENSO, models with meridionally broader τ^x responses during ENSO also tended to exhibit more eastward SSTA propagation and a stronger projected amplification of ENSO SSTAs in the future (Merryfield, 2006). Nearly all models underestimate the meridional width of the τ^x response (Capotondi et al., 2006), which suggests that the future amplification of ENSO in the real world might be even stronger than suggested by the models (Vecchi & Wittenberg, 2010).

A third example of an emergent constraint relates to future changes in the climatological equatorial Pacific zonal and meridional SST gradients, which as described above are key controls on the atmospheric response to ECT SSTAs during ENSO events. Huang & Ying (2015) found that CMIP5 models with weaker and more realistic

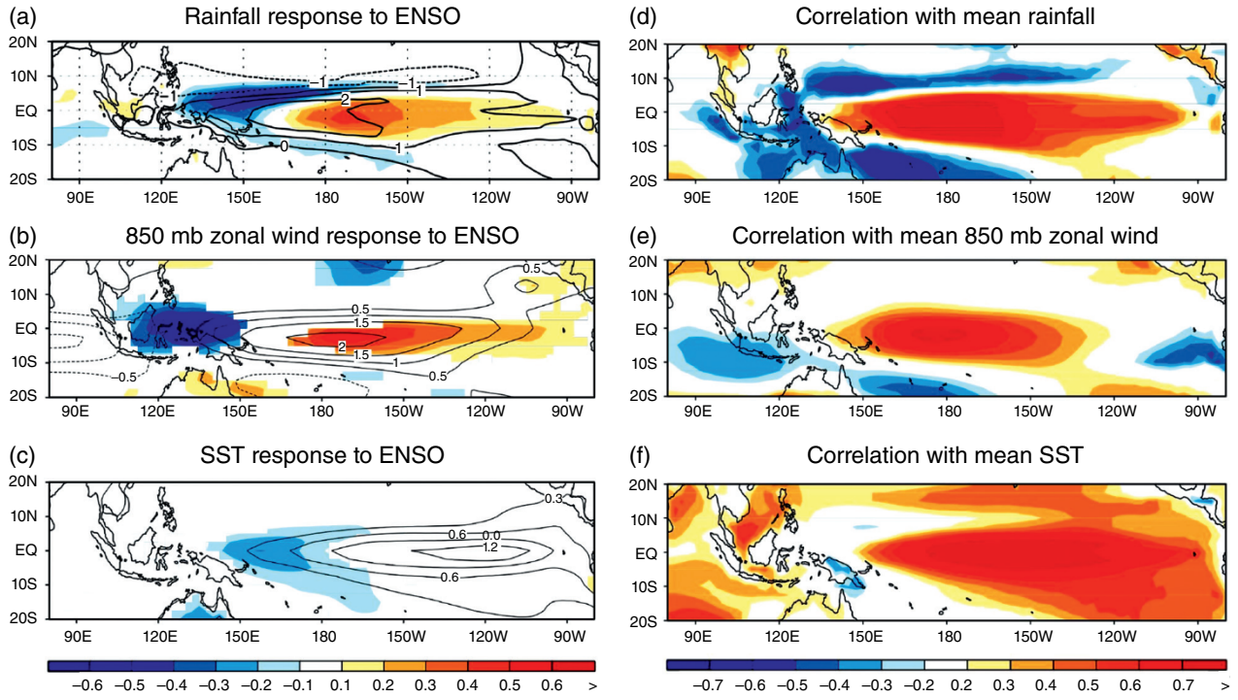

Figure 9.5 Links between ENSO anomaly patterns and the background climatology among the CMIP5 models. For each model, various anomaly fields are regressed onto SSTAs averaged over the Niño-3.4 region (170°W–120°W, 5°S–5°N). Contours in the left column indicate these multimodel mean anomaly regressions (i.e. ENSO responses) for (a) rainfall (mm day^{-1} K^{-1}), (b) 850 hPa zonal wind (m s^{-1} K^{-1}), and (c) SST (K K^{-1}). The leading intermodel principal component of ENSO precipitation anomalies, P_1, is then used to stratify the models. Shading in the left column shows the intermodel regressions of ENSO anomaly patterns onto P_1 for each variable. Right column shows intermodel correlations of climatological mean fields with P_1 for (d) rainfall, (e) 850 hPa zonal wind, and (f) SST. Thus, a CMIP5 model with a more eastward-shifted equatorial Pacific rainfall response during El Niño (east-west dipole pattern in (a)) also tends to have a more eastward-shifted (b) zonal wind response and (c) SST response, along with (d) more eastward- and equatorward-shifted tropical Pacific mean rainfall, (e) weaker mean easterly trade winds along the equator, and (f) warmer SST in the equatorial Pacific cold tongue. Adapted from Figures 2, 4, and 5 of Ham and Kug (2015).

climatological ECTs also tended to project more future weakening of the climatological SST gradients, suggesting that the future climatology might be more El Niño–like than most models suggest, and more conducive to enhanced eastward and equatorward shifts of atmospheric convection during future El Niño events. Ying & Huang (2016a, 2016b) found that this relationship stemmed from both atmospheric and oceanic sources: (i) models with stronger and more realistic damping of SSTAs (due to cloud shading) tended to *inhibit* future SST warming in the western equatorial Pacific; and (ii) models with weaker and more realistic upwelling in the eastern equatorial Pacific tended to *enhance* SST warming in the east, as this reduced the inhibition of warming associated with anthropogenically enhanced thermal stratification of the tropical Pacific upper ocean.

Further candidates for emergent constraints appear in the CMIP5 analysis of C. Chen et al. (2017), who found robust relationships between the El Niño/La Niña SSTA asymmetries in historical simulations and the projected future changes in those asymmetries.

It remains an open question whether emergent constraints diagnosed from a limited set of biased climate models offer a reliable way to infer future sensitivities of the real world. Key questions are whether the existing models are a sufficiently diverse, independent, and representative sample of the relationships between biases and sensitivities, or whether deficiencies that are common to all of the models (e.g. limited resolution in the ocean and atmosphere) may reduce the utility of these emergent constraints.

9.4.4. Prospects for Improving ENSO Simulations

ENSO simulations are affected by an inability of CGCMs to fully capture several important processes involving small scales that are difficult to represent adequately with present atmosphere/ocean resolutions.

WWBs. As described in more detail in this chapter and others, westerly wind bursts (WWBs, also known as westerly wind events or WWEs) are a key stochastic forcing for ENSO. At the onset of El Niño, WWBs tend to strengthen and expand eastward as the warm pool expands eastward, thus representing a broadband multiplicative stochastic forcing for ENSO (Vecchi et al., 2006; Gebbie et al., 2007; Zavala-Garay et al., 2008; Levine et al., 2016; Puy et al., 2016; Levine & Jin, 2017; Thual et al., 2016; Capotondi et al., 2018). WWBs contribute to ENSO's seasonality, its asymmetry between El Niño and La Niña, and its diversity from event to event (Lengaigne et al., 2004; Levine et al., 2016; Hayashi & Watanabe, 2017). Unfortunately, many CGCMs have difficulty reproducing the observed properties of the WWBs as well as the MJO (Ahn et al., 2017; Feng & Lian, 2018), which provides the large-scale context for WWBs to occur (Puy et al., 2017).

Barrier layers. In the warm pool region, heavy rain can cap the sea surface with a shallow lens of fresh water, leading to increased density stratification and formation of a "barrier layer" beneath the mixed layer that inhibits deep mixing. As momentum from the wind stress is deposited into a thinner surface layer, the barrier layer can enhance the response of the surface currents during WWBs, leading to greater eastward acceleration of the surface currents and stronger zonal advective–induced warming of the central Pacific at the onset of El Niño (Maes et al., 2005; Maes & Belamari, 2011; Zhu et al., 2014). Unfortunately, most AGCMs lack sufficient horizontal resolution to simulate the strong WWBs and strong rain events, and most OGCMs lack the upper-ocean vertical resolution to properly represent barrier layers and their associated strong surface currents. Thus, CGCMs might not fully capture the impacts of barrier layers on the WWB-induced multiplicative stochastic forcing of ENSO.

TIWs. In the real world, vigorous tropical instability waves (TIWs) stir water across the northern and southern flanks of the ECT. This stirs warm water equatorward at the surface, enhances ocean heat uptake from the atmosphere off-equator, and induces strong transient shears that enhance mixing at the base of the mixed layer within the ECT (Jochum et al., 2005; Jochum & Murtugudde, 2006; Menkes et al., 2006; Holmes et al., 2014; Holmes & Thomas, 2015). Together, these effects can act to thermally stratify the ECT and reduce vertical mixing near the surface (Ray et al., 2018a, 2018b), potentially affecting ENSO indirectly by altering the Ekman and thermocline feedbacks. TIWs can also influence ENSO more directly. TIWs affect ENSO asymmetries, since they are more active during La Niña than El Niño (Nagura et al., 2008; Imada & Kimoto, 2012; R.-H. Zhang, 2016), and TIWs also cause fluctuations in surface wind stress over the ECT, which may constitute an additional stochastic forcing for ENSO (Jochum et al., 2007). Most CGCMs fail to fully represent TIWs and their effects on the ECT heat budget, due to coarse OGCM resolution and poor simulation of wind stress curls and associated upper-ocean zonal jets for the tropical Pacific, which weaken the subsurface shears and TIW generation (Marchesiello et al., 2011; Graham, 2014; Wittenberg et al., 2018).

Numerous studies have demonstrated improved simulations of the tropical Pacific climatology and ENSO as a result of improved model resolution in the atmosphere and ocean components (Roberts et al., 2009). Wittenberg et al. (2018) found that refining the atmospheric horizontal grid from 200 km to 25 km improved the simulated tropical Pacific climatological upper-ocean currents and temperatures, due to reduced biases in simulated rainfall and wind stress cyclonicity off-equator. This greatly improved the simulation of ENSO and its impacts (Delworth et al., 2012; Vecchi et al., 2013; Jia et al., 2015; Krishnamurthy et al., 2015, 2016; W. Zhang et al., 2016; Murakami et al., 2015; Yang et al., 2015). Refining the oceanic horizontal grid from 100 km to 10 km also leads to greatly improved simulation of the Pacific TIWs and their equatorward heat transport (Marchesiello et al., 2011; Griffies et al., 2015). There is also hope that refined vertical grids could help, e.g. by improving the atmospheric representation of tropical Pacific boundary layer moisture and cloudiness (especially near the coast of South America), and by improving the oceanic representation of upper-ocean barrier layers, shears, and vertical mixing. Sufficient temporal resolution is important as well: studies have shown that resolving the diurnal cycle of solar radiation is important for the simulated time-mean ocean mixed layer and surface fluxes (Stockdale et al., 1998; Bernie et al., 2008; Weihs & Bourassa, 2014).

As enhanced atmospheric resolutions gradually reduce the need for convective parameterization, many model biases (e.g. the double ITCZ) that are sensitive to those parameterizations may diminish. At present though, the resources required for seasonal forecasts and centennial projections currently limit atmospheric grids to about 50 km, well short of the 2–3 km needed to explicitly resolve deep convection. Atmospheric and coupled model simulations of the tropical Pacific continue to show strong sensitivity to parameterizations of atmospheric convection and clouds. This frequently leads to compromises during model development, since the combination of parameters that produces a realistic climatology or realistic ENSO may be very different from the combination that yields realistic MJO variability and tropical cyclone statistics.

A key aspect of atmospheric convection that has been shown to affect ENSO simulations is the representation

of convective momentum transport (CMT), namely, the vertical transport of horizontal momentum that results from subgrid scale vertical motions advecting on the strong vertical shears associated with the Pacific Walker circulation. During El Niño, an eastward and equatorward shift of tropical Pacific deep convection leads to increased CMT over the equatorial central Pacific, bringing upper-level westerly momentum down toward the surface boundary layer where it can amplify and meridionally broaden the existing westerly wind anomalies. This amplifies the Bjerknes feedback and slows the poleward discharge of equatorial ocean heat content, which in turn amplifies ENSO and lengthens its period (Wittenberg, 2002; Wittenberg et al., 2006; Capotondi et al., 2006; Kim et al., 2008; Neale et al., 2008).

In ocean models, several parameterizations affect the simulation of tropical Pacific climate and ENSO. Parameterized vertical mixing affects the intensity and depth of the equatorial thermocline and undercurrent, as well as ENSO's subsurface feedbacks (Meehl et al., 2001; Wilson, 2000; Canuto et al., 2004; Noh et al., 2005; Ray et al., 2018a, 2018b). The parameterization of lateral viscosity affects the intensity of the equatorial undercurrent and its associated shears, which in turn affect the intensity of Pacific TIWs and their equatorward heat transport (Stockdale et al., 1998; Griffies et al., 2005; Wittenberg et al., 2018). The parameterization of solar penetration through the water column, which depends on both the ocean turbidity and the optical model used for radiative transfer through the ocean, can also strongly affect the ECT and ENSO, by modifying the structure of the equatorial thermocline, via both local and nonlocal effects (Murtugudde et al., 2002; Anderson et al., 2007, 2009; Lengaigne et al., 2007).

9.5. CHALLENGES AND OPPORTUNITIES

The ability of CGCMs to simulate ENSO continues to improve, offering exciting opportunities for research, forecasting, understanding past variations, and projecting the future behavior of ENSO and its global impacts. Many GCMs have also now evolved into more comprehensive Earth system models that simulate atmospheric chemistry, ocean biogeochemistry, land vegetation, dust, fire, and the carbon cycle, enabling pioneering new research and applications related to ENSO's impacts on air quality, ecosystems, agriculture, and fisheries. Other GCMs have pushed toward higher resolution in the atmosphere and ocean, enabling seamless simulations of weather and climate with applications to ENSO's impacts on tropical cyclones, severe weather, coastal communities, and regional extremes.

The research and modeling communities also continue to become better organized. CMIPs are enabling groundbreaking research by the academic community, by coordinating multimodel experiments that support periodic assessments by the Intergovernmental Panel on Climate Change (IPCC). The quality and diversity of observational and reanalysis constraints for models are improving and are now being provided in formats that are convenient for modelers to use, e.g. via the Obs4MIPs project (Ferraro et al., 2015). Freely available diagnostic frameworks are enabling more rapid assessment of simulations, and efforts are well underway to support those activities and the broader climate community by providing comprehensive sets of ENSO diagnostics and metrics for models (Guilyardi et al., 2016).

There are many ways that models could be better leveraged to yield insight into ENSO's mechanisms, sensitivities, and predictability. Key foci are (i) the atmosphere response to SSTAs, (ii) surface wind stress and heat flux feedbacks over the tropical Pacific, (iii) the upwelling and vertical mixing near the equator, and (iv) the upper-ocean heat budgets for both the background climatology and ENSO. Long control runs and large ensembles can be used to illuminate ENSO's diversity and interdecadal modulation, and perturbed-physics ensembles can be used to systematically probe the sensitivity of ENSO to model parameters. EMICs and statistical emulators can be used as diagnostics of models, enabling more robust intercomparisons and evaluations against short observational records. Seasonal forecasts could be used to better understand the seeds and amplifiers of model biases and initialization shocks. Model analogs could be employed to assess the fundamental predictability of ENSO to provide a baseline of skill against which to evaluate initialized forecasts. Emergent constraints can provide insight into the relationship between model biases and model sensitivities and possibly leverage the intermodel diversity to yield more reliable projections of future ENSO behavior.

Further improvement of ENSO simulations will rely on several factors. First, modeling advances must be supported by improved observational constraints. These should include more reliable, representative, and diverse observations from moorings, satellites, ships, and drifters, as well as maintenance of the long-term climate records needed to assess simulated decadal variability and sensitivities to external forcings. Improving observational constraints for ENSO simulations and forecasts is a major thrust of the Tropical Pacific Observing System 2020 (TPOS2020) project (Cravatte et al., 2016; Kessler et al., 2019). Also essential are statistical and GCM-based reanalyses that reconcile the diverse observations, fill gaps between them, and impute variables that are not directly observed; such reanalyses are essential for evaluating the detailed processes (e.g. heat budgets) and multidecadal behavior of ENSO in the models. Efforts to rescue and digitize historical observations, such as the Global Oceanographic Data Archaeology and Rescue

Project (GODAR), are also essential to support these reanalyses. Paleo constraints should not be overlooked, as they provide a unique perspective on the longer-term variability of ENSO. As proxy records become ever more numerous, consistent, and better understood, they can support multiproxy reanalyses extending deep into the past and may even be able to improve understanding of the early part of the instrumental era via merged reanalyses involving both proxy and instrumental observations (e.g., Emile-Geay et al., 2013, Freund et al., 2019).

Second, it will be essential to maintain and advance a robust hierarchy of models, including simple conceptual models, EMICs, ocean-only and atmosphere-only simulations, statistical and empirical models, and comprehensive CGCMs (free, nudged, flux-adjusted, or partially-coupled). Quality documentation and software archiving (e.g. via github) are also essential to make EMICs and simple models easily available to the community. Investments in intellectual, software infrastructure, and computing resources are needed to support improved model resolution, more realistic processes and parameterizations, larger ensembles to characterize extremes, and more diverse and creative sets of experiments with the GCMs, as well as improved foundations in ENSO theory for the simpler models.

Based on past experience, the return on these investments, from improved predictions and projections that benefit global economies and societies to better fundamental understanding of Earth's climate variations, is likely to be exceptional.

ACKNOWLEDGMENTS

We thank the editors and three anonymous reviewers for their careful reading of the manuscript, and their help in improving it. EG is funded by the Centre National de la Recherche Scientifique (CNRS), ML is funded by the Institut de Recherche pour le Développement (IRD), and they both acknowledge the support of the Belmont Forum project GOTHAM, under grant ANR-15-JCLI-0004-01 and the Agence Nationale de la Recherche project ARISE, under grant ANR-18-CE01-0012. AC was supported by the NASA Physical Oceanography Program (Award NNX15AG46G).

REFERENCES

Abellán, E., S. McGregor, & M. H. England (2017). Analysis of the southward wind shift of ENSO in CMIP5 models. *J. Climate*, *30*, 2415–2435, https://doi.org/10.1175/JCLI-D-16-0326.1

AchutaRao, K., & K. Sperber (2006). ENSO simulations in coupled ocean-atmosphere models: Are the current models better? *Climate Dyn.*, *27*, 1–16.

An, S.-I., & Jin, F.-F. (2001). Collective role of thermocline and zonal advective feedbacks in the ENSO mode. *J. Climate*, *14*(16), 3421–3432.

An, S.-I., & F.-F. Jin (2004). Nonlinearity and asymmetry of ENSO. *J. Climate*, *17*, 2399–2412.

An, S.-I., & B. Wang (2000). Interdecadal change of the structure of ENSO mode and its impact on the ENSO frequency. *J. Climate*, *13*, 2044-2055. doi:10.1175/1520-0442%282000%29013<2044%3AICOTSO>2.0.CO;2

An, S., Y. Ham, J. Kug, F. Jin, & I. Kang (2005). El Niño–La Niña asymmetry in the coupled model intercomparison project simulations. *J. Climate*, *18*, 2617–2627. doi:10.1175/JCLI3433.1

Ahn, M. S., D. Kim, K. R. Sperber, I.-S. Kang, E. Maloney, D. Waliser, & H. Hendon (2017). MJO simulation in CMIP5 climate models: MJO skill metrics and process-oriented diagnosis. *Climate Dyn.*, *49*, 4023–4045. doi:10.1007/s00382-017-3558-4

Anderson, W. G, A. Gnanadesikan, R. Hallberg, J. Dunne, & B. L. Samuels (2007). Impact of ocean color on the maintenance of t D. J. Vimont (2017). Characterizing unforced multi-decadal variability of ENSO: A case study with the GFDL CM2.1 coupled GCM. *Climate Dyn., 49*(7–8), 2845–2862. doi: 10.1007/s00382-016-3477-9

Barnett, T. P., Graham, N., Pazan, S., White, W., Latif, M., & Flügel, M. (1993). ENSO and ENSO-related predictability. Part I: Prediction of equatorial Pacific sea surface temperature with a hybrid coupled ocean–atmosphere model. *Journal of Climate*, *6*(8), 1545–1566.

Barnston, A.G., M. K. Tippett, M. L. L'Heureux, S. Li, & D. G. DeWitt (2012). Skill of real-time seasonal ENSO model predictions during 2002–11: Is Our capability increasing? *Bull. Amer. Meteor. Soc.*, *93*, 631–651. https://doi.org/10.1175/BAMS-D-11-00111.1

Battisti, D. S., & A. C. Hirst, 1989). Interannual variability in the tropical atmosphere–ocean system: Influence of the basic state and ocean geometry. *J. Atmos. Sci.*, *46*, 1678–1712.

Bellenger, H., E. Guilyardi, J. Leloup, J. Lengaigne, & J. Vialard (2014). ENSO representation in climate models: from CMIP3 to CMIP5. *Climate Dyn.*, *42*, 1999–2018. doi:10.1007/s00382-013-1783-z

Bernie, D. J., E. Guilyardi, G. Madec, J. M. Slingo, S. J. Woolnough, & J. Cole (2008). Impact of resolving the durnal cycle in an ocean-atmosphere GCM. Part 2: A diurnally coupled CGCM. *Climate Dyn., 31*, 909–925. doi: 10.1007/s00382-008-0429-z

Bianucci, M., A. Capotondi, S. Merlino, & R. Mannella (2018). Estimate of the average timing for strong El Niño events using the recharge oscillator model with a multiplicative perturbation. *Chaos*, *28*, 103118.

Bony S., K. Lau, & Y. C. Sud (1997). Sea surface temperature and large-scale circulation influences on tropical greenhouse effect and cloud radiative forcing. *J. Climate*, *10*, 2055–2077.

Brown J. N., & A. V. Fedorov (2010). How much energy is transferred from the winds to the thermocline on ENSO timescales? *J. Clim.*, *23*, 1563–1580.

Brown J., A. Fedorov, & E. Guilyardi (2011). How well do coupled models replicate the energetics of ENSO? *Clim. Dyn.*, *36*, 2147–2158.

Burgers G., F.-F. Jin, & G. J. van Oldenborgh (2005). The simplest ENSO recharge oscillator. *Geophys. Res. Lett.*, *32*, L13706. doi:10.1029/2005GL022951

Burls, N. J., & A. V. Fedorov (2014). What controls the mean east–west sea surface temperature gradient in the equatorial Pacific: The role of cloud albedo. *J. Climate*, *27*, 2757–2778. doi:10.1175/JCLI-D-13-00255.1

Cai, W., et al. (2014). Increasing frequency of extreme El Niño events due to greenhouse warming. *Nat. Clim. Change*, *4*, 111–116. doi:10.1038/NCLIMATE2100

Cai, W., G. Wang, B. Dewitte, L. Wu, A. Santoso, K. Takahashi, et al. (2018). Increased variability of eastern Pacific El Niño under greenhouse warming. *Nature*, *564*, 201–206.

Canuto, V. M., A. Howard, Y. Cheng, & R. L. Miller (2004). Latitude-dependent vertical mixing and the tropical thermocline in a global OGCM. *Geophys. Res. Lett.*, *31*, L16305. doi:10.1029/2004GL019891

Capotondi, A. (2013). ENSO diversity in the NCAR CCSM4. *J. Geophys. Res.*, *118*, 4755–4770.

Capotondi, A., & P. D. Sardeshmukh (2017). Is El Niño really changing? *Geophys. Res. Lett.*, *44*, 8548–8556. doi:10.1002/2017GL074515

Capotondi, A., M. A. Alexander, C. Deser, & M. McPhaden (2005). Anatomy and decadal evolution of the Pacific subtropical-tropical cells (STCs). *J. Climate*, *18*, 3739–3758.

Capotondi, A., A. Wittenberg, & S. Masina (2006). Spatial and temporal structure of tropical Pacific interannual variability in 20th century coupled simulations. *Ocean Modelling*, *15*, 274–298. doi: 10.1016/j.ocemod.2006.02.004

Capotondi, A., Y.-G. Ham, A. T. Wittenberg, & J.-S. Kug (2015a). Climate model biases and El Niño Southern Oscillation (ENSO) simulation. *U.S. CLIVAR Variations*, *13*(1), 21–25.

Capotondi, A., A. T. Wittenberg, et al. (2015b). Understanding ENSO diversity. *Bull. Amer. Meteor. Soc.*, *96*, 921–938. doi: 10.1175/BAMS-D-13-00117.1

Capotondi, A., P. D. Sardeshmukh, & L. Ricciardulli (2018). The nature of the stochastic wind forcing of ENSO. *J. Climate*, *31*, 8081–8099. https://doi.org/10.1175/JCLI-D-17-0842.1

Chen, D., S. E. Zebiak, A. J. Busalacchi, & M. A. Cane (1995). An improved procedure for EI Nino forecasting: Implications for predictability. *Science*, *269*(5231), 1699–1702.

Chen, D., M. A. Cane, A. Kaplan, S. E. Zebiak, & D. Huang (2004). Predictability of El Niño over the past 148 years. *Nature*, *428*(6984), 733.

Chen, C., M. A. Cane, A. T. Wittenberg, & D. Chen (2017). ENSO in the CMIP5 simulations: Life cycles, diversity, and responses to climate change. *J. Climate*, *30*(2), 775–801. doi: 10.1175/JCLI-D-15-0901.1

Chiodi, A. M., & D.E. Harrison (2017). Observed El Niño SSTA development and the effects of easterly and westerly wind events in 2014/15. *J. Climate*, *30*, 1505–1519, https://doi.org/10.1175/JCLI-D-16-0385.1

Choi, J., S.-I. An, J.-S. Kug, & S.-W. Yeh (2011). The role of mean state on changes in El Niño flavor. *Clim. Dyn.*, *37*, 1205–1215.

Choi, J., S.-I. An, & S.-W. Yeh (2012). Decadal amplitude modulation of two types of ENSO and its relationship with the mean state. *Clim. Dyn.*, *28*, 2631–2644.

Choi, J., S. An, S. Yeh, & J. Yu (2013a). ENSO-like and ENSO-induced tropical Pacific decadal variability in CGCMs. *J. Climate*, *26*, 1485–1501. doi:10.1175/JCLI-D-12-00118.1

Choi, K.-Y., G. A. Vecchi, & A. T. Wittenberg (2013b). ENSO transition, duration and amplitude asymmetries: Role of the nonlinear wind stress coupling in a conceptual model. *J. Climate*, *26*, 9462–9476. doi: 10.1175/JCLI-D-13-00045.1

Choi, K.-Y., G. A. Vecchi, & A. T. Wittenberg (2015). Nonlinear zonal wind response to ENSO in the CMIP5 models: Roles of the zonal and meridional shift of the ITCZ/SPCZ and the simulated climatological precipitation. *J. Climate*, *28*, 8556–8573. doi: 10.1175/JCLI-D-15-0211.1

Clarke, A. J., S. Van Gorder, & G. Colantuono (2007). Wind stress curl and ENSO discharge/recharge in the equatorial Pacific. *J. Phys. Oceanogr.*, *37*(4), 1077–1091.

Claussen, M., L. Mysak, A. Weaver, et al. (2002). *Climate Dynamics*, *18*, 579. https://doi.org/10.1007/s00382-001-0200-1

Collins, M., S.-I. An, W. Cai, A. Ganachaud, E. Guilyardi, F.-F. Jin, et al. (2010). The impact of global warming on the tropical Pacific and El Niño. *Nature Geoscience*, *3*, 391–397. doi: 10.1038/ngeo868

Collins M., M. Sutherland, L. Bouwer, S.-M. Cheong, T. Frölicher, H. Jacot Des Combes, et al. (2019). Extremes, abrupt changes and managing risk. In H.-O. Pörtner, D.C. Roberts, V. Masson-Delmotte, P. Zhai, M. Tignor, E. Poloczanska, et al. (Eds.), *IPCC special report on the ocean and cryosphere in a changing climate*. IPCC.

Cravatte, S., B. Kessler, N. Smith, S. Wijffels, L. Yu, K. Ando, et al. (2016). First report of TPOS 2020. GOOS-215 (200 pp.) [Available online at http://tpos2020.org/first-report.] doi: 10.13140/RG.2.2.28674.07363

Delecluse, P., M. Davey, Y. Kitamura, S. G. H. Philander, M. Suarez, & L. Bengtsson, 1998). TOGA review paper: Coupled general circulation modeling of the tropical Pacific. *J. Geophys. Res.*, *103*, 14,357–14,373.

Delworth, T. L., A. Rosati, W. Anderson, A. J. Adcroft, V. Balaji, R. Benson, et al. (2012). Simulated climate and climate change in the GFDL CM2.5 high-resolution coupled climate model. *J. Climate*, *25*, 2755–2781. doi: 10.1175/JCLI-D-11-00316.1

de Szoeke, S.P., & S. Xie (2008). The tropical eastern Pacific seasonal cycle: Assessment of errors and mechanisms in IPCC AR4 coupled ocean–atmosphere general circulation models. *J. Climate*, *21*, 2573–2590. doi:10.1175/2007JCLI1975.1

Di Lorenzo, E., G. Liguori, N. Schneider, J. C. Furtado, B. T. Anderson, & M. A. Alexander (2015). ENSO and meridional modes: A null hypothesis for Pacific climate variability. *Geophys. Res. Lett.*, *42*, 9440–9448. doi:10.1002/2015GL066281

DiNezio, P. N., B. P. Kirtman, A. C. Clement, S.-K. Lee, G. A. Vecchi, & A. Wittenberg (2012). Mean climate controls on the simulated response of ENSO to increasing greenhouse gases. *J. Climate*, *25*, 7399–7420. doi: 10.1175/JCLI-D-11-00494.1

Ding, H., M. Newman, M. A. Alexander, & A. T. Wittenberg (2018). Skillful climate forecasts of the tropical Indo-Pacific Ocean using model-analogs. *J. Climate*, *31*(14), 5437–5459. doi:10.1175/JCLI-D-17-0661.1

Ding, H., M. Newman, M. A. Alexander, & A. T. Wittenberg (2019). Diagnosing secular variations in retrospective ENSO

seasonal forecast skill using CMIP5 model-analogs. *Geophys. Res. Lett.*, *46*(3), 1721–1730. doi:10.1029/2018GL080598

Ding, H., M. Newman, M. A. Alexander, & A. T. Wittenberg (2020). Relating CMIP5 model biases to seasonal forecast skill in the tropical Pacific. *Geophys. Res. Lett.*, *47*(5), e2019GL086765. doi:10.1029/2019GL086765

Dommenget, D., & Y. Yu (2016). The seasonally changing cloud feedbacks contribution to the ENSO seasonal phase-locking. *Climate Dynamics*, *47*(12), 3661–3672.

Dommenget, D., T. Bayr, & C. Frauen (2013). Analysis of the non-linearity in the pattern and time evolution of El Niño Southern Oscillation. *Climate Dyn.*, *40*, 2825–2847. doi:10.1007/s00382-012-1475-0

Eisenman, I., L. Yu, & E. Tziperman (2005). Westerly wind bursts: ENSO's tail rather than the dog? *Journal of Climate*, *18*(24), 5224–5238.

Emile-Geay, J., K. M. Cobb, M. E. Mann, & A. T. Wittenberg (2013). Estimating central equatorial Pacific SST variability over the past millennium. *Part II: Reconstructions and implications. J. Climate 26*, 2329–2352.

Eyring, V., S. Bony, G. A. Meehl, C. A. Senior, B. Stevens, R. J. Stouffer, & K. E. Taylor (2016). Overview of the Coupled Model Intercomparison Project Phase 6 (CMIP6) experimental design and organization. *Geosci. Model Dev.*, *9*, 1937–1958, https://doi.org/10.5194/gmd-9-1937-2016

Fedorov, A. V., & S. G. Philander (2000). Is El Niño changing? *Science*, *288*, 1997–2002.

Fedorov, A. V., & S. G. Philander (2001). A stability analysis of tropical ocean–atmosphere interactions: Bridging measurements and theory for El Niño. *J. Climate*, *14*, 3086–3101.

Fedorov, A.V., S. L. Harper, S. G. Philander, B. Winter, & A. Wittenberg (2003). How predictable is El Niño? *Bull. Amer. Meteor. Soc.*, *84*, 911–920. https://doi.org/10.1175/BAMS-84-7-911

Feng, J., & T. Lian (2018). Assessing the relationship between MJO and equatorial Pacific WWBs in observations and CMIP5 models. *J. Climate*, *31*, 6393–6410. https://doi.org/10.1175/JCLI-D-17-0526.1

Ferraro, R., D. E. Waliser, P. Gleckler, K. E. Taylor, & V. Eyring (2015). Evolving Obs4MIPs to support Phase 6 of the Coupled Model Intercomparison Project (CMIP6). *Bull. Amer. Meteor. Soc.*, *96*, ES131–ES133. https://doi.org/10.1175/BAMS-D-14-00216.1

Flato, G., J. Marotzke, B. Abiodun, P. Braconnot, S. C. Chou, W. Collins, et al. (2013). Evaluation of climate models. In Stocker, T. F., D. Qin, G.-K. Plattner, M. Tignor, S. K. Allen, J. Boschung, et al. (Eds.), *Climate change 2013: The physical science basis. Contribution of Working Group I to the Fifth Assessment Report of the Intergovernmental Panel on Climate Change (IPCC AR5)*. Cambridge University Press.

Freund, M. B., Henley, B. J., Karoly, D. J., McGregor, H. V., Abram, N. J. & Dommenget, D. (2019). Higher frequency of central Pacific El Niño events in recent decades relative to past centuries. *Nature Geoscience*, *6*, 450–455. doi:10.1038/s41561-019-0353-3

Gebbie, G., I. Eisenman, A. Wittenberg, & E. Tziperman (2007). Modulation of westerly wind bursts by sea surface temperature: A semistochastic feedback for ENSO. *J. Atmos. Sci.*, *64*, 3281–295. doi: 10.1175/JAS4029.1

Gill, A. E. (1980) Some simple solutions for heat-induced tropical circulation. *Q J R Meteor Soc, 106*, 447–462. https://doi.org/10.1002/qj.49710644905

Gillett, N. P., H. Shiogama, B. Funke, G. Hegerl, R. Knutti, K. Matthes, et al. (2016). The Detection and Attribution Model Intercomparison Project (DAMIP v1.0) contribution to CMIP6. *Geosci. Model Dev., 9,* 3685–3697.

Graham, T. (2014). The importance of eddy permitting model resolution for simulation of the heat budget of tropical instability waves. *Ocean Modelling*, *79*, 21–32. doi:10.1016/j.ocemod.2014.04.005

Graham, F. S., J. N. Brown, C. Langlais, S. J. Marsland, A. T. Wittenberg, & N. J. Holbrook (2014). Effectiveness of the Bjerknes stability index in representing ocean dynamics. *Climate Dyn.*, *43*, 2399–2414. doi: 10.1007/s00382-014-2062-3

Graham, F. S., J. N. Brown, A. T. Wittenberg, & N. J. Holbrook (2015). Reassessing conceptual models of ENSO. *J. Climate*, *28*, 9121–9142. doi: 10.1175/JCLI-D-14-00812.1

Graham, F. S., A. T. Wittenberg, J. N. Brown, S. J. Marsland, & N. J. Holbrook (2017). Understanding the double peaked El Niño in coupled GCMs. *Climate Dyn.*, *48*(5), 2045–2063. doi: 10.1007/s00382-016-3189-1

Griffies, S. M., A. Gnanadesikan, K. W. Dixon, J. P. Dunne, et al. (2005). Formulation of an ocean model for global climate simulations. *Ocean Sci.*, *1*, 45-79. doi:10.5194/os-1-45-2005

Griffies, S. M., M. Winton, W. G. Anderson, R. Benson, T. L. Delworth, C. O. Dufour, et al. (2015). Impacts on ocean heat from transient mesoscale eddies in a hierarchy of climate models. *J. Climate*, *28*, 952–977. doi: 10.1175/JCLI-D-14-00353.1

Guckenheimer J., A. Timmermann, H. Dijkstra, & A. Roberts (2017). (Un)predictability of strong El Niño events. *Dynamics and Statistics of the Climate System*, *2*(1). dzx004, https://doi.org/10.1093/climsys/dzx004

Guilyardi, E. (2006). El Niño–mean state–seasonal cycle interactions in a multi-model ensemble. *Clim. Dyn.*, *26*, 329–348, doi: 10.1007/s00382-005-0084-6

Guilyardi E., S. Gualdi, J. M. Slingo, A. Navarra, P. Delecluse, J. Cole, et al. (2004). Representing El Niño in coupled ocean-atmosphere GCMs: The dominant role of the atmospheric component. *J. Climate*, *17*, 4623–4629.

Guilyardi, E., A. Wittenberg, A. Fedorov, M. Collins, C. Wang, A. Capotondi, et al. (2009). Understanding El Niño in ocean-atmosphere general circulation models: Progress and challenges. *Bull. Amer. Meteor. Soc.*, *90*, 325–340. doi: 10.1175/2008BAMS2387.1

Guilyardi, E., H. Bellenger, M. Collins, S. Ferrett, W. Cai, & A. Wittenberg (2012a). A first look at ENSO in CMIP5. *CLIVAR Exchanges*, *17*, 29–32. ISSN: 1026-0471.

Guilyardi, E., W. Cai, M. Collins, A. Fedorov, F.-F. Jin, A. Kumar, et al. (2012b). New strategies for evaluating ENSO processes in climate models. *Bull. Amer. Met. Soc.*, *93*, 235–238. doi: 10.1175/BAM S-D-11-00106.1

Guilyardi, E., A. Wittenberg, M. Balmaseda, W. Cai, M. Collins, M. J. McPhaden, et al. (2016). Fourth CLIVAR workshop on the evaluation of ENSO processes in climate models: ENSO in a changing climate. *Bull. Amer. Meteor. Soc.*, *97*(5), 817–820. doi: 10.1175/BAMS-D-15-00287.1

Haarsma, R. J., M. J. Roberts, P. L. Vidale, C. A. Senior, A. Bellucci, Q. Bao, et al. (2016). High Resolution Model Intercomparison Project (HighResMIP v1.0) for CMIP6. *Geoscientific Model Development*, *9*, 11, 4185–4208.

Ham, Y.-G., & J.-S. Kug (2012). How well do current climate models simulate two types of El Nino? *Climate Dyn.*, *39*, 383–398. doi:10.1007/s00382-011-1157-3

Ham, Y.-G., & J.-S. Kug (2015). Improvement of ENSO simulation based on intermodel diversity. *J. Climate*, *28*, 998–1015. doi:10.1175/JCLI-D-14-00376.1

Hayashi, M., & M. Watanabe (2017). ENSO complexity induced by state dependence of westerly wind events. *J. Climate*, *30*, 3401–3420. doi:10.1175/JCLI-D-16-0406.1

He, J., N. C. Johnson, G. A. Vecchi, B. Kirtman, A. T. Wittenberg, & S. Sturm (2018). Precipitation sensitivity to local variations in tropical sea surface temperature. *J. Climate*, *31*(22), 9225–9238. doi:10.1175/JCLI-D-18-0262.1

Heinze, C., Eyring, V., Friedlingstein, P., Jones, C., Balkanski, Y., Collins, et al. (2019). ESD Reviews: Climate feedbacks in the Earth system and prospects for their evaluation. *Earth Syst. Dynam.*, *10*, 379-452. https://doi.org/10.5194/esd-10-379-2019 (2019.

Held, I. M. (2005). The gap between simulation and understanding in climate modeling. *Bull. Amer. Meteor. Soc.*, *86*, 1609–1614.

Holmes, R. M., & L. N. Thomas (2015). The modulation of equatorial turbulence by tropical instability waves in a regional ocean model. *J. Phys. Oceanogr.*, *45*, 1155–1173. doi:10.1175/JPO-D-14-0209.1

Holmes, R., L. Thomas, L. Thompson, & D. Darr (2014). Potential vorticity dynamics of tropical instability vortices. *J. Phys. Oceanogr.*, *44*, 995–1011. doi:10.1175/JPO-D-13-0157.1

Hu, S., & Fedorov, A. V. (2016). Exceptionally strong easterly wind burst stalling El Niño of 2014. *Pnas*, *113*(8), 2005–2010. http://doi.org/10.1007/s00704-008-0069-6

Huang, P., & D. Chen (2017). Enlarged asymmetry of tropical Pacific rainfall anomalies induced by El Niño and La Niña under global warming. *J. Climate*, *30*, 1327–1343. doi:10.1175/JCLI-D-16-0427.1

Huang, P., & J. Ying (2015). A multimodel ensemble pattern regression method to correct the tropical Pacific SST change patterns under global warming. *J. Climate*, *28*, 4706–4723. doi:10.1175/JCLI-D-14-00833.1

Hung, M., J. Lin, W. Wang, D. Kim, T. Shinoda, & S. J. Weaver (2013). MJO and convectively coupled equatorial waves simulated by CMIP5 Climate Models. *J. Climate*, *26*, 6185–6214, https://doi.org/10.1175/JCLI-D-12-00541.1

Imada, Y., & M. Kimoto (2012). Parameterization of tropical instability waves and examination of their impact on ENSO Characteristics. *J. Climate*, *25*, 4568–4581, doi:10.1175/JCLI-D-11-00233.1

Izumo, T., Lengaigne, M., Vialard, J., Suresh, I., & Planton, Y. (2018). On the physical interpretation of the lead relation between the warm water volume and the El Niño Southern Oscillation. *Climate Dynamics*, *52*, 2923–2942. https://doi.org/10.1007/s00382-018-4313-1

Jia, L., X. Yang, G. A. Vecchi, R. G. Gudgel, T. L. Delworth, A. Rosati, et al. (2015). Improved seasonal prediction of temperature and precipitation over land in a high-resolution GFDL climate model. *J. Climate*, *28*, 2044–2062. doi: 10.1175/JCLI-D-14-00112.1

Jin, F. (1997). An equatorial ocean recharge paradigm for ENSO. Part I: Conceptual model. *J. Atmos. Sci., 54*, 811–829. https://doi.org/10.1175/1520-0469(1997)054<0811:AEORPF>2.0.CO;2

Jin, F.-F. (2001). Low-frequency modes of tropical ocean dynamics. *J. Climate*, *14*(18), 3874–3881.

Jin, F. F., & J. D. Neelin (1993). Modes of interannual tropical ocean–atmosphere interaction: A unified view. *Part I: Numerical results. J. Atmos. Sci*, *50*, 3477–3503.

Jin F-F, S. T. Kim, & L. Bejarano (2006). A coupled-stability index for ENSO. *Geophys. Res. Lett.*, *33*, L23708, doi:10.1029/2006GL027221

Jin, F.-F., L. Lin, A. Timmermann, & J. Zhao (2007). Ensemble-mean dynamics of the ENSO recharge oscillator under state-dependent stochastic forcing. *Geophys.Res.Lett.*, *34*. doi:10.1029/2006GL027372

Jochum, M. & R. Murtugudde (2006). Temperature advection by tropical instability waves. *J. Phys. Oceanogr.*, *36*, 592–605. doi:10.1175/JPO2870.1

Jochum, M., et al. (2005). The impact of horizontal resolution on the tropical heat budget in an Atlantic Ocean Model. *J. Climate*, *18*, 841–851. doi:10.1175/JCLI-3288.1

Jochum, M., et al. (2007). Tropical atmospheric variability forced by oceanic internal variability. *J. Climate*, *20*, 765–771. doi:10.1175/JCLI4044.1

Kageyama, M., P. Braconnot, S. P. Harrison, A. M. Haywood, J. Jungclaus, B. L. Otto-Bliesner, et al. (2018). PMIP4-CMIP6: The contribution of the Paleoclimate Modelling Intercomparison Project to CMIP6. *Geosci. Model Dev.*, *11*, 1033–1057. https://doi.org/10.5194/gmd-11-1033-2018

Kajtar, J. B., A. Santoso, M. H. England, & W. Cai (2017). Tropical climate variability: Interactions across the Pacific, Indian, and Atlantic Oceans. *Climate Dyn.*, *48*, 2173–2190. doi:10.1007/s00382-016-3199-z

Kamenkovich, I. V., & E. S. Sarachik (2004). Reducing errors in temperature and salinity in an ocean model forced by restoring boundary conditions. *J. Phys. Oceanogr.*, *34*, 1856–1869. doi:10.1175/1520-0485(2004)034<1856:REITAS>2.0.CO;2

Karamperidou, C., M. A. Cane, U. Lall, & A. T. Wittenberg (2014). Intrinsic modulation of ENSO predictability viewed through a local Lyapunov lens. *Climate Dyn.*, *42*, 253–270. doi: 10.1007/s00382-013-1759-z

Kessler, W. S., S. E. Wijffels, S. Cravatte, N. Smith, A. Kumar, Y. Fujii, et al. (2019). Second Report of TPOS 2020. GOOS-234, 265 pp. Available online at http://tpos2020.org/project-reports/second-report. doi: 10.13140/RG.2.2.17161.29289

Khodri M., T. Izumo, J. Vialard, S. Janicot, C. Cassou, M. Lengaigne, et al. (2017). Tropical explosive volcanic eruptions can trigger El Niño by cooling tropical Africa. *Nature Communications*, *8*, 778. doi:10.1038/s41467-017-00755-6

Kim, D., J.-S. Kug, I.-S. Kang, F.-F. Jin, & A. T. Wittenberg (2008). Tropical Pacific impacts of convective momentum transport in the SNU coupled GCM. *Climate Dyn.*, *31*, 213–226. doi: 10.1007/s00382-007-0348-4

Kim, S. T. & F.-F. Jin (2011). An ENSO stability analysis. Part II: Results from the twentieth and twenty-first century simulations of the CMIP3 models. *Climate Dynamics*, *36*, 1609–1627.

Kirtman, B. P., & Zebiak, S. E. (1997). ENSO simulation and prediction with a hybrid coupled model. *Monthly Weather Review*, *125*(10), 2620–2641.

Kleeman, R. (1993). On the dependence of hindcast skill on ocean thermodynamics in a coupled ocean–atmosphere model. *J. Climate*, *6*, 2012–2033.

Kleeman, R., & S. B. Power (1994). Limits to predictability in a coupled ocean-atmosphere model due to atmospheric noise. *Tellus*, *46A*, 529–540.

Kociuba, G., & S. B. Power (2015). Inability of CMIP5 models to simulate recent strengthening of the Walker Circulation: Implications for projections. *J. Climate*, *28*, 20–35. doi:10.1175/JCLI-D-13-00752.1

Krishnamurthy, L., G. Vecchi, R. Msadek, A. Wittenberg, T. Delworth, & F. Zeng (2015). The seasonality of the Great Plains Low-Level Jet and ENSO relationship. *J. Climate*, *28*, 4525–4544. doi: 10.1175/JCLI-D-14-00590.1

Krishnamurthy, L., G. A. Vecchi, R. Msadek, H. Murakami, A. Wittenberg, & F. Zeng (2016). Impact of strong ENSO on regional tropical cyclone activity in a high-resolution climate model in the North Pacific and North Atlantic. *J. Climate*, *29*, 2375–2394. doi: 10.1175/JCLI-D-0468.1

Kröger, J., & F. Kucharski (2011). Sensitivity of ENSO characteristics to a new interactive flux correction scheme in a coupled GCM. *Climate Dyn.*, *36*, 119–137. doi:10.1007/s00382-010-0759-5

Kug, J.-S., J. Choi, S.-I. An, F.-F. Jin, & A. T. Wittenberg (2010). Warm pool and cold tongue El Niño events as simulated by the GFDL CM2.1 coupled GCM. *J. Climate*, *23*, 1226–1239. doi: 10.1175/2009JCLI3293.1

Kug, J.-S., Y.-G. Ham, J.-Y. Lee, & F.-F. Jin (2012). Improved simulation of two types of El Nino in CMIP5 models. *Environ. Res. Lett.*, *7*, 034002. doi:10.1088/1748-9326/7/3/034002

Large, W. G., & G. Danabasoglu (2006). Attribution and impacts of upper-ocean biases in CCSM3. *J. Climate*, *19*, 2325–2346. doi:10.1175/JCLI3740.1

Larson, S. M., & Kirtman, B. P. (2015). Revisiting ENSO Coupled Instability Theory and SST error growth in a fully coupled model. *Journal of Climate*, *28*(12), 4724–4742. http://doi.org/10.1175/JCLI-D-14-00731.1

Latif M., & A. Villwock (1990). Interannual variability in the tropical Pacific as simulated in coupled ocean-atmosphere models. *Journal of Marine Systems*, *1*, 51–60, https://doi.org/10.1016/0924-7963(90)90119-U

Lee, S.-K., A. T. Wittenberg, D. B. Enfield, S. J. Weaver, C. Wang, & R. M. Atlas (2016). U.S. regional tornado outbreaks and their links to spring ENSO phases and North Atlantic SST variability. *Environ. Res. Lett., 11*(4), 044008. doi: 10.1088/1748-9326/11/4/044008

Lee, S.-K., H. Lopez, E.-S. Chung, P. DiNezio, S.-W. Yeh, & A. T. Wittenberg (2018). On the fragile relationship between El Niño and California rainfall. *Geophys. Res. Lett.*, *45*(2), 907–915. doi:10.1002/2017GL076197

Lengaigne M., J. P. Boulanger, C. Menkes, P. Delecluse, & J. Slingo (2004). Westerly wind events in the tropical Pacific and their influence on the coupled ocean–atmosphere system: A review. In C. Wang, S.-P. Xie, & J. A. Carton (Eds.), *Earth's climate: The ocean–atmosphere interaction (pp. 49–69)*. Amer. Geophys. Union.

Lengaigne M., C. Menkes, O. Aumont, T. Gorgues, L. Bopp, J.-M. André, & G. Madec (2007). Influence of the oceanic biology on the tropical Pacific climate in a Coupled General Circulation Model. *Climate Dynamics,* 28: 503–516, doi:10.1007/s00382-006-0200-2

Levine, A., & F. F. Jin (2010). Noise-induced instability in the ENSO recharge oscillator. *J. Atm. Sci.*, *67*(2):529–542.

Levine, A. F. Z., & F. F. Jin (2017). A simple approach to quantifying the noise–ENSO interaction. *Part I: Deducing the state-dependency of the windstress forcing using monthly mean data. Climate Dyn.*, *48*, 1–18. doi:10.1007/s00382-015-2748-1

Levine, A. F. Z., F. F. Jin, & M. J. McPhaden (2016). Extreme noise–Extreme El Niño: How state-dependent forcing creates El Niño–La Niña Asymmetry. *J. Climate. 29*, 5483-5499. doi: 10.1175/JCLI-D-16-0091.1

Liguori, G., & E. Di Lorenzo (2018). Meridional modes and increasing Pacific decadal variability under anthropogenic forcing. *Geophys. Res. Lett.*, *45*, 983–991. doi:10.1002/2017GL076548

Lin, J. (2007). The double-ITCZ problem in IPCC AR4 coupled GCMs: Ocean–atmosphere feedback analysis. *J. Climate*, *20*, 4497–4525. https://doi.org/10.1175/JCLI4272.1

Lin, R., F. Zheng, & X. Dong (2018). ENSO frequency asymmetry and the Pacific decadal oscillation in observations and 19 CMIP5 models. *Adv. Atmos. Sci.*, *35*, 495–506. doi:10.1007/s00376-017-7133-z

Liu, Z., & E. Di Lorenzo (2018). Mechanisms and predictability of Pacific decadal variability. *Current Climate Change Reports.* https://doi.org/10.1007/s40641-018-0090-5

Lloyd J., E. Guilyardi, H. Weller, & J. Slingo (2009). The role of atmosphere feedbacks during ENSO in the CMIP3 models. *Atmos. Sci. Let.*, *10*, 170–176.

Lloyd J., E. Guilyardi, H. Weller, (2012). The role of atmosphere feedbacks during ENSO in the CMIP3 models. *Part III: The shortwave flux feedback. J. Clim.*, *25*, 4275–4293.

Luo J.-J., et al. (2012). Indian Ocean warming modulates Pacific climate change. *Proc. Natl. Acad. Sci.*, *109*, 18701–18706. doi:10.1073/pnas.1210239109

Lutsko, N. J., & K. Takahashi (2018). What can the internal variability of CMIP5 models tell us about their climate sensitivity? *J. Climate*, *31*, 5051–5069. https://doi.org/10.1175/JCLI-D-17-0736.1

Lyu, K., X. Zhang, J. A. Church, & J. Hu (2015). Quantifying internally generated and externally forced climate signals at regional scales in CMIP5 models. *Geophys. Res. Lett.*, *42*, 9394–9403. doi: 10.1002/2015GL065508

Maes, C., & S. Belamari (2011). On the impact of salinity barrier layer in the Pacific ocean mean state and ENSO. *Sci. Online Lett. Atmos.*, *7*, 97-100. doi:10.2151/sola.2011-025

Maes, C., J. Picaut, & S. Belamari (2005). Importance of the salinity barrier layer for the buildup of El Niño. *J. Climate*, *18*, 104–118. doi:10.1175/JCLI-3214.1

Magnan, A. K., M. Garschagen, J-P. Gattuso, J. E. Hay, N. Hilmi, E. Holland, et al. (2019). Integrative cross-chapter box on low-lying islands and coasts. In H.-O. Pörtner, D. C. Roberts, V. Masson-Delmotte, P. Zhai, M. Tignor, E. Poloczanska, et al., *IPCC special report on the ocean and cryosphere in a changing climate*. IPCC.Magnusson, L., M. Alonso-Balmaseda, & F. Molteni (2013a). On the dependence

of ENSO simulation on the couped model mean state. *Climate Dyn., 41,* 1509–1525. doi:10.1007/s00382-012-1574-y

Magnusson, L., M. Alonso-Balmaseda, S. Corti, F. Molteni, & T. Stockdale (2013). Evaluation of forecast strategies for seasonal and decadal forecasts in presence of systematic model errors. *Climate Dyn.*, *41*, 2393–2409. doi:10.1007/s00382-012-1599-2

Manganello, J. V., & B. Huang (2009). The influence of systematic errors in the Southeast Pacific on ENSO variability and prediction in a coupled GCM. *Climate Dyn.*, *32*, 1015–1034. doi:10.1007/s00382-008-0407-5

Marchesiello, P., X. Capet, C. Menkes, & S. C. Kennan (2011). Submesoscale dynamics in tropical instability waves. *Ocean Modelling*, *39*, 31–46. doi:10.1016/j.ocemod.2011.04.011

Marzeion, B., Timmermann, A., Murtugudde, R., & Jin, F. F. (2005). Biophysical feedbacks in the tropical Pacific. *Journal of Climate*, *18*(1), 58–70.

McGregor, S., M. F. Stuecker, J. B. Kajtar, M. H. England, & M. Collins (2018). Model tropical Atlantic biases underpin diminished Pacific decadal variability. *Nat. Clim. Change*, *8*, 493–498. doi:10.1038/s41558-018-0163-4

McPhaden, M. J., & D. Zhang (2002). Slowdown of the meridional overturning circulation in upper Pacific Ocean. *Nature*, *415*, 603.

Meehl, G. A., P. R. Gent, J. M. Arblaster, B. L. Otto-Bliesner, E. C. Brady, & A. Craig (2001). Factors that affect the amplitude of El Nino in global coupled climate models. *Climate Dyn.*, *17*, 515–526. doi:10.1007/PL00007929

Menkes, C., et al. (2006). A modeling study of the impact of tropical instability waves on the heat budget of the eastern equatorial Pacific. *J. Phys. Oceanogr.*, *36*, 847–865. doi:10.1175/JPO2904.1

Merryfield, W. J. (2006). Changes to ENSO under CO2 doubling in a multimodel ensemble. *J. Climate*, *19*, 4009–4027, https://doi.org/10.1175/JCLI3834.1

Moore, A. M., & R. Kleeman (1999). Stochastic forcing of ENSO by the intraseasonal oscillation. *Journal of Climate*, *12*(5), 1199–1220.

Murakami, H., G. A. Vecchi, S. Underwood, T. L. Delworth, A. T. Wittenberg, W. G. Anderson, et al. (2015). Simulation and prediction of category 4 and 5 hurricanes in the high-resolution GFDL HiFLOR coupled climate model. *J. Climate*, *28*, 9058–9079. doi: 10.1175/JCLI-D-15-0216.1

Murtugudde, R., J. Beauchamp, C. R. McClain, M. Lewis, & A. J. Busalacchi (2002). Effects of penetrative radiation on the upper tropical ocean circulation. *J. Climate*, *15*, 470–486. doi:10.1175/1520-0442(2002)015<0470:EOPROT>2.0.CO;2

Nagura, M., K. Ando, & K. Mizuno (2008). Pausing of the ENSO cycle: A case study from 1998 to 2002. *J. Climate*, *21*, 342–363. doi:10.1175/2007JCLI1765.1

Neale, R. B., et al. (2008). The impact of convection on ENSO: From a delayed oscillator to a series of events. *J. Climate*, *21*, 5904–5924. doi:10.1175/2008JCLI2244.1

Neelin, J. D. (1990). A hybrid coupled general circulation model for El Niño studies. *Journal of the Atmospheric Sciences*, *47*(5), 674–693.

Neelin, J. D., & F. Jin (1993). Modes of interannual tropical ocean–atmosphere interaction—A unified view. *Part II: Analytical results in the weak-coupling limit. J. Atmos. Sci.*, *50*, 3504–3522, https://doi.org/10.1175/1520-0469(1993)050<3504:MOITOI>2.0.CO;2

Neelin, J. D., D. S. Battisti, A. C. Hirst, F.-F. Jin, Y. Wakata, T. Yamagata, & S. E. Zebiak (1998). ENSO theory. *J. Geophys. Res.*, *103*(C7), 14261–14290. doi:10.1029/97JC03424

Neske, S., & S. McGregor (2018). Understanding the warm water volume precursor of ENSO events and its interdecadal variation. *Geophysical Research Letters*, *45*, 1577–1585. https://doi.org/10.1002/2017GL076439

Newman, M., et al. (2011). Natural variation in ENSO flavors. *Geophys. Res. Lett.*, *38*, L14705. doi: 10.1029/2011GL047658

Newman, M., M. A. Alexander, T. R. Ault, K. M. Cobb, C. Deser, E. Di Lorenzo, et al. (2016). The Pacific decadal oscillation, revisited. *J. Climate*, *29*, 4399–4427. doi:10.1175/JCLI-D-15-0508.1

Newman, M., A. T. Wittenberg, L. Cheng, G. P. Compo, & C. A. Smith (2018). The extreme 2015/16 El Niño, in the context of historical climate variability and change. Section 4 of "Explaining extreme events of 2016 from a climate perspective." *Bull. Amer. Meteor. Soc.*, *99*(1), S16–S20. doi: 10.1175/BAMS-D-17-0116.1

Noh, Y., Y. J. Kang, T. Matsuura, & S. Iizuka (2005). Effect of the Prandtl number in the parameterization of vertical mixing in an OGCM of the tropical Pacific. *Geophys. Res. Lett.*, *32*, L23609. doi:10.1029/2005GL024540.

Ogata, T., S.-P. Xie, A. Wittenberg, & D.-Z. Sun (2013). Interdecadal amplitude modulation of El Niño/Southern Oscillation and its impacts on tropical Pacific decadal variability. *J. Climate*, *26*, 7280–7297. doi: 10.1175/JCLI-D-12-00415.1

O'Neill, B. C., C. Tebaldi, D. van Vuuren, V. Eyring, P. Fridelingstein, G. Hurtt, et al. (2016). The Scenario Model Intercomparison Project (ScenarioMIP) for CMIP6. *Geosci. Model Dev.*, *9*, 3461–3482.

Pan, X., B. Huang, & J. Shukla (2011). Sensitivity of the tropical Pacific seasonal cycle and ENSO to changes in mean state induced by a surface heat flux adjustment in CCSM3. *Climate Dyn.*, *37*, 325–341. doi:10.1007/s00382-010-0923-y

Penland, C., & P. D. Sardeshmukh (1995). The optimal growth of tropical sea surface temperature anomalies. *J. Climate*, *8*, 1999–2024.

Philander, S. G., T. Yamagata, & R.C. Pacanowski (1984). Unstable air-sea interactions in the tropics. *J. Atmos. Sci.*, *41*, 604–613, https://doi.org/10.1175/1520-0469(1984)041<0604:UASIIT>2.0.CO;2

Picaut, J., F. Masia, and Y. du Penhoat (1997). An advective-reflective conceptual model for the oscillatory nature of the ENSO. *Science*, *277*(5326), 663–666.

Planton Y., J. Vialard, E. Guilyardi, M. Lengaigne, & T. Izumo (2018). Western Pacific oceanic heat content: A better predictor of La Niña than of El Niño. *Geophys. Res. Lett.* https://doi.org/10.1029/2018gl079341

Power, S. B., et al. (2013). Robust twenty-first-century projections of El Nino and related precipitation variability. *Nature*, *502*, 541–545. doi:10.1038/nature12580

Power, S. B., F. Delage, G. Wang, I. Smith, & G. Kociuba (2017). Apparent limitations in the ability of CMIP5 climate models to simulate recent multi-decadal change in surface temperature: Implications for global temperature projections. *Climate Dyn.*, *49*, 53–69. doi:10.1007/s00382-016-3326-x

Predybaylo, E., G. Stenchikov, A. T. Wittenberg, & F. Zeng (2017). Impacts of a Pinatubo-scale volcanic eruption on ENSO. *J. Geophys. Res. Atmos.*, *122*, 925–947. doi: 10.1002/2016JD025796

Puy, M., J. Vialard, M. Lengaigne, & E. Guilyardi (2016). Modulation of equatorial Pacific westerly/easterly wind events by the Madden–Julian oscillation and convectively-coupled Rossby waves. *Climate Dyn.*, *46*, 2155–2178. doi:10.1007/s00382-015-2695-x

Puy M., J. Vialard, M. Lengaigne, E. Guilyardi, P. N. Di Nezio, A. Voldoire, et al. (2017). Influence of westerly wind events stochasticity on El Niño amplitude: The case of 2014 vs. 2015. *Clim. Dyn*., doi:10.1007/s00382-017-3938-9

Rashid, H. A., & A. C. Hirst (2016). Investigating the mechanisms of seasonal ENSO phase locking bias in the ACCESS coupled model. *Clim Dyn*, *46*, 1075–1090. https://doi.org/10.1007/s00382-015-2633-y

Rashid, H. A., A. C. Hirst, & S. J. Marsland (2016). An atmospheric mechanism for ENSO amplitude changes under an abrupt quadrupling of CO2 concentration in CMIP5 models. *Geophys. Res. Lett.*, *43*, 1687–1694. doi:10.1002/2015GL066768

Ray, S., A. T. Wittenberg, S. M. Griffies, & F. Zeng (2018a). Understanding the equatorial Pacific cold tongue time-mean heat budget, Part I: Diagnostic framework. *J. Climate*, *31*(24), 9965–9985. doi:10.1175/JCLI-D-18-0152.1

Ray, S., A. T. Wittenberg, S. M. Griffies, & F. Zeng (2018b). Understanding the equatorial Pacific cold tongue time-mean heat budget, Part II: Evaluation of the GFDL-FLOR coupled GCM. *J. Climate*, *31*(24), 9987–10011. doi:10.1175/JCLI-D-18-0153.1

Ren, H. L., J. Zuo, F. F. Jin, & M. Stuecker (2016). ENSO and annual cycle interaction: The combination mode representation in CMIP5 models. *Clim Dyn*, *46*, 3753. https://doi.org/10.1007/s00382-015-2802-z

Roberts, M. J., A. Clayton, M. Demory, J. Donners, P. L. Vidale, W. Norton, et al. (2009). Impact of resolution on the tropical Pacific circulation in a matrix of coupled models. *J. Climate*, *22*, 2541–2556. https://doi.org/10.1175/2008JCLI2537.1

Santoso, A., H. Hendon, A. Watkins, S. Power, et al. (2019). Dynamics and predictability of the El Niño-Southern Oscillation: An Australian perspective on progress and challenges. *Bull. Amer. Meteor. Soc.*, *100*, 403–420. doi:10.1175/BAMS-D-18-0057.1

Schopf, P. S., & M. J. Suarez (1988). Vacillations in a coupled ocean–atmosphere system. *J. Atmos. Sci.*, *45*, 3283–3287.

Schopf, P. S., & M. J. Suarez (1990). Ocean wave dynamics and the time scale of ENSO. *J. Phys. Oceanogr., 20*, 629–645. https://doi.org/10.1175/1520-0485(1990)020<0629:OWDATT>2.0.CO;2

Small, R. J., E. Curchitser, K. Hedstrom, B. Kauffman, & W. G. Large (2015). The Benguela upwelling system: Quantifying the sensitivity to resolution and coastal wind representation in a global climate model. *J. Climate*, *28*, 9409–9432. doi:10.1175/JCLI-D-15-0192.1

Song, F., & G. J. Zhang (2016). Effects of southeastern Pacific sea surface temperature on the double-ITCZ bias in NCAR CESM1. *J. Climate*, *29*, 7417–7433. doi:10.1175/JCLI-D-15-0852.1

Spencer, H., R. Sutton, & J. M. Slingo (2007). El Niño in a coupled climate model: Sensitivity to changes in mean state induced by heat flux and wind stress corrections. *J. Climate*, *20*, 2273–2298. doi:10.1175/JCLI4111.1

Stein, K., A. Timmerman, N. Schneider, F.-F. Jin, & M. Stuecker (2014). ENSO seasonal synchronization theory. *J. Climate*, *27*, 5285–5310. doi:10.1175/JCLI-D-13-00525.1

Stevenson, S., B. Fox-Kemper, M. Jochum, B. Rajagopalan, & S.G. Yeager (2010). ENSO model validation using wavelet probability analysis. *J. Climate*, *23*, 5540–5547. doi:10.1175/2010JCLI3609.1

Stockdale, T. N., A. J. Busalacchi, D. E. Harrison, & R. Seager (1998). Ocean modeling for ENSO. *J. Geophys. Res.*, *103*, 14325–14355. doi:10.1029/97JC02440

Stuecker, M. F., A. Timmermann, F.-F. Jin, S. McGregor, & H.-L. Re (2013). A combination mode of the annual cycle and the El Niño/Southern Oscillation. *Nat Geosci 6*, 540–544.

Stuecker, M. F., A. Timmermann, F.-F. Jin, Y. Chikamoto, W. Zhang, A. T. Wittenberg, et al. (2017). Revisiting ENSO/Indian Ocean dipole phase relationships. *Geophys. Res. Lett.*, *44*(5), 2481–2492. doi:10.1002/2016GL072308

Suarez, M. J., & P. S. Schopf (1988). A delayed action oscillator for ENSO. *J. Atm. Sci.*, *45*(21), 3283–3287.

Sun D. Z., Y. Yu, & T. Zhang (2009). Tropical water vapor and cloud feedbacks in climate models: A further assessment using coupled simulations. *J. Climate*, *22*, 1287–1304.

Syu, H. H., J. D. Neelin, & D. Gutzler (1995). Seasonal and interannual variability in a hybrid coupled GCM. *Journal of Climate*, *8*(9), 2121–2143.

Takahashi, K., & B. Dewitte (2016). Strong and moderate nonlinear El Niño regimes. *Clim Dyn*, *46*, 1627. https://doi.org/10.1007/s00382-015-2665-3

Takahashi, K., C. Karamperidou, and B. Dewitte (2018). A theoretical model of strong and moderate el Niño regimes. *Clim. Dyn.* doi:10.1007/s00382-018-4100-z

Taschetto, A. S., A. S. Gupta, N. C. Jourdain, A. Santoso, C. C. Ummenhofer, & M. H. England (2014). Cold tongue and warm pool ENSO events in CMIP5: Mean state and future projections. *J. Climate*, *27*, 2861–2885. https://doi.org/10.1175/JCLI-D-13-00437.1

Terray P., S. Masson, C. Prodhomme, M. Koll Roxy & K. P. Sooraj (2015). Impacts of Indian and Atlantic oceans on ENSO in a comprehensive modeling framework. *Climate Dynamics*, *46*(7–8), 2507–2533. doi: 10.1007/s00382-015-2715-x

Thomas, M. D., & A. V. Fedorov (2017). The eastern subtropical Pacific origin of the equatorial cold bias in climate models: A Lagrangian perspective. *J. Climate*, *30*, 5885–5900. doi:10.1175/JCLI-D-16-0819.1

Thual, S., A. J. Majda, N. Chen, & S. N. Stechmann (2016). Simple stochastic model for El Niño with westerly wind bursts. *Proc. Nat. Acad. Sci*, *113*, 10245–10250. doi:10.1073/pnas.1612002113

Timmerman, A., & F. Jin. (2003). A nonlinear theory for El Nino bursting. *J. Atmos. Sci.*, *60*, 152–165.

Timmermann, A., S.-I. An, J.-S. Kug, F.-F. Jin, W. Cai, A. Capotondi, et al. (2018). El Niño-Southern Oscillation complexity. *Nature*, *559* (7715), 535–545. doi:10.1038/s41586-018-0252-6

Tziperman, E., L. Stone, M. A. Cane, & H. Jarosh (1994). El Niño chaos: Overlapping of resonances between the seasonal

cycle and the Pacific ocean–atmosphere oscillator. *Science*, *264*, 72– 74.

Vannière B., E. Guilyardi, G. Madec, F. J. Doblas-Reyes, & S. Woolnough (2013). Using seasonal hindcasts to understand the origin of the equatorial cold tongue bias in CGCMs and its impact on ENSO. *Clim. Dyn.*, *40*, 963–981, doi: 10.1007/s00382-012-1429-6

Vannière, B., E. Guilyardi, T. Toniazzo, G. Madec, & S. Woolnough (2014). A systematic approach to identify sources of tropical SST errors in coupled models using the adjustment of initialised experiments. *Clim. Dyn.*, *43*, 2261–2282. doi: 10.1007/s00382-014-2051-6

van Oldenborgh, G.J. (2000). What Caused the Onset of the 1997–98 El Niño?. *Mon. Wea. Rev.*, *128*, 2601–2607, doi:10.1175/1520-0493(2000)128<2601:WCTOOT>2.0.CO;2

van Oldenborgh, G. J., S. Philip, & M. Collins (2005). El Niño in a changing climate: A multi-model study. *Ocean Sci.*, *1*, 81–95.

Vecchi, G. A., & A. T. Wittenberg (2010). El Niño and our future climate: Where do we stand? *Wiley Interdisciplinary Reviews: Climate Change*, *1*, 260–270. doi: 10.1002/wcc.33

Vecchi, G. A., A. T. Wittenberg, & A. Rosati (2006). Reassessing the role of stochastic forcing in the 1997-8 El Niño. *Geophys. Res. Lett.*, *33*, L01706. doi: 10.1029/2005GL024738

Vecchi, G. A., R. Msadek, W. Anderson, Y.-S. Chang, T. Delworth, K. Dixon, et al. (2013). Multiyear predictions of North Atlantic hurricane frequency: Promise and limitations. *J. Climate*, *26*, 5337–5357. doi: 10.1175/JCLI-D-12-00464.1

Vecchi, G. A., T. Delworth, H. Murakami, S. D. Underwood, A. T. Wittenberg, F. Zeng, et al. (2019). Tropical cyclone sensitivities to CO2 doubling: Roles of atmospheric resolution, synoptic variability and background climate changes. *Climate Dyn.*, *53*, 5999–6033.

Vialard J., C. Menkes, J. P. Boulanger, E. Guilyardi, P. Delecluse, M. McPhaden & G. Madec (2001). Oceanic mechanisms driving the SST during the 1997-98 El Niño. *J. Phys. Oceanog.*, *31*, 1649–1675.

Vijayeta, A., & D. Dommenget (2018). An evaluation of ENSO dynamics in CMIP simulations in the framework of the recharge oscillator model. *Clim Dyn*, *51*, 1753. https://doi.org/10.1007/s00382-017-3981-6

Wang, C., & J. Picaut (2004). Understanding ENSO physics: A review. In C. Wang, S.-P. Xie, and J. A. Carton (Eds.), *Earth's climate: The ocean-atmosphere interaction* (Geophysical Monograph Series, Vol. *147*, pp. 21–48). Washington, DC: AGU.

Wang, T., & J.-P. Miao (2018). Twentieth-century Pacific Decadal Oscillation simulated by CMIP5 coupled models. *Atmos. Ocean. Sci. Lett.*, *11*, 94–101. doi:10.1080/16742834.2017.1381548

Watanabe, M., & A. T. Wittenberg (2012). A method for disentangling El Niño-mean state interaction. *Geophys. Res. Lett.*, *39*, L14702. doi: 10.1029/2012GL052013

Watanabe, M., J.-S. Kug, F.-F. Jin, M. Collins, M. Ohba, & A. T. Wittenberg (2012). Uncertainty in the ENSO amplitude change from the past to the future. *Geophys. Res. Lett.*, *39*, L20703. doi: 10.1029/2012GL053305

Weihs, R. R., & M. A. Bourassa (2014). Modeled diurnally varying sea surface temperatures and their influence on surface heat fluxes. *J. Geophys. Res. Oceans*, *119*, 4101–4123, doi:10.1002/2013JC009489

Wieners, C. E., et al. (2017). The influence of the Indian Ocean on ENSO stability and flavor. *J. Climate*, *30*, 2601–2620. doi:10.1175/JCLI-D-16-0516.1

Wilson, S. G. (2000). How ocean vertical mixing and accumulation of warm surface water influence the "sharpness" of the equatorial thermocline. *J. Climate*, *13*, 3638–3656. doi:10.1175/1520-0442(2000)013<3638:HOVMAA>2.0.CO;2

Wittenberg, A. T. (2002). ENSO response to altered climates. Ph.D. thesis, Princeton University. 475 pp. doi: 10.13140/RG.2.1.1777.8403/1

Wittenberg, A. T. (2009). Are historical records sufficient to constrain ENSO simulations? *Geophys. Res. Lett.*, *36*, L12702. doi: 10.1029/2009GL038710

Wittenberg, A. T. (2015). Low-frequency variations of ENSO. *U.S. CLIVAR Variations*, *13*(1), 26–31.

Wittenberg, A. T., A. Rosati, N.-C. Lau, & J. J. Ploshay (2006). GFDL's CM2 global coupled climate models, *Part III: Tropical Pacific climate and ENSO. J. Climate*, *19*, 698–722. doi: 10.1175/JCLI3631.1

Wittenberg, A. T., A. Rosati, T. L. Delworth, G. A. Vecchi, & F. Zeng (2014). ENSO modulation: Is it decadally predictable? *J. Climate*, *27*, 2667–2681. doi: 10.1175/JCLI-D-13-00577.1

Wittenberg, A. T., G. A. Vecchi, T. L. Delworth, A. Rosati, W. Anderson, W. F. Cooke, et al. (2018). Improved simulations of tropical Pacific annual-mean climate in the GFDL FLOR and HiFLOR coupled GCMs. *J. Adv. Model. Earth Syst.,10*, 3176–3220. doi:10.1029/2018MS001372

Xie, S.-P., C. Deser, G. A. Vecchi, J. Ma, H. Teng, & A. T. Wittenberg (2010). Global warming pattern formation: Sea surface temperature and rainfall. *J. Climate*, *23*, 966–986. doi: 10.1175/2009JCLI3329.1

Yang, X., G. A. Vecchi, R. G. Gudgel, T. L. Delworth, S. Zhang, A. Rosati, et al. (2015). Seasonal predictability of extratropical storm tracks in GFDL's high-resolution climate prediction model. *J. Climate*, *28*, 3592–3611. doi: 10.1175/JCLI-D-14-00517.1

Yeh, S.-W., J.-S. Kug, B. Dewitte, M.-H. Kwon, B. P. Kirtman, & F.-F. Jin (2009). El Niño in a changing climate. *Nature*, *461*. doi:10.1038/nature08316

Ying, J., & P. Huang (2016a). Cloud-radiation feedback as a leading source of uncertainty in the tropical Pacific SST warming pattern in CMIP5 models. *J. Climate*, *29*, 3867–3881. doi:10.1175/JCLI-D-15-0796.1

Ying, J., & P. Huang (2016b). The large-scale ocean dynamical effect on uncertainty in the tropical Pacific SST warming pattern in CMIP5 models. *J. Climate*, *29*, 8051–8065. doi:10.1175/JCLI-D-16-0318.1

Yu, Y., D. Dommenget, C. Frauen, G. Wang, & S. Wales (2015). ENSO dynamics and diversity resulting from the recharge oscillator interacting with the slab ocean. *Clim Dyn.* doi: 10.1007/s00382-015-2667-1

Zavala-Garay, J., C. Zhang, A. M. Moore, A. T. Wittenberg, M. J. Harrison, A. Rosati, et al. (2008). Sensitivity of hybrid ENSO models to unresolved atmospheric variability. *J. Climate*, *21*, 3704-3721. doi: 10.1175/2007JCLI1188.1

Zebiak, S. E., & M. A. Cane (1987). A model El Niño–Southern Oscillation. *Mon. Wea. Rev.*, *115*, 2262–2278.

Zhang, R.-H. (2016). A modulating effect of Tropical Instability Wave (TIW)-induced surface wind feedback in a hybrid coupled model of the tropical Pacific. *J. Geophys. Res. Oceans*, *121*, 7326–7353. doi: 10.1002/2015JC011567

Zhang, R.-H., Zebiak, S. E., Kleeman, R., & Keenlyside, N. (2003). A new intermediate coupled model for El Nino simulation and prediction. *Geophysical Research Letter*, *30*(19), 2012. https://doi.org/10.1029/2003GL018010

Zhang, R., F. Tian, A. J. Busalacchi, & X. Wang (2019). Freshwater flux and ocean chlorophyll produce nonlinear feedbacks in the tropical Pacific. *J. Climate*, *32*, 2037–2055, https://doi.org/10.1175/JCLI-D-18-0430.1

Zhang, T., & D. Sun (2014). ENSO asymmetry in CMIP5 models. *J. Climate*, *27*, 4070–4093. doi:10.1175/JCLI-D-13-00454.1

Zhang, W., F.-F. Jin, M. F. Stuecker, A. T. Wittenberg, A. Timmermann, H.-L. Ren, et al. (2016). Unraveling El Niño's impact on the East Asian monsoon and Yangtze River summer flooding. *Geophys. Res. Lett.*, *43* (21), 11375-11382. doi: 10.1002/2016GL071190

Zheng W., P. Braconnot, E. Guilyardi, U. Merkel & Y. Yu (2008). ENSO at 6ka and 21ka from ocean-atmosphere coupled model simulations. *Clim. Dyn.*, *30*, 745–762.

Zhu, J., & A. Kumar (2018). Influence of surface nudging on climatological mean and ENSO feedbacks in a coupled model. *Climate Dyn*, *50*, 571–586. doi:10.1007/s00382-017-3627-8

Zhu, J., B. Huang, R.-H. Zhang, Z.-Z. Hu, A. Kumar, M. A. Balmaseda, et al. (2014). Salinity anomaly as a trigger for ENSO events. *Nature Sci. Rep.*, *4*, 6821. doi: 10.1038/srep06821